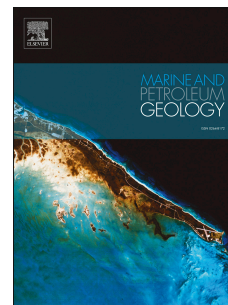# Journal Pre-proof

A new and working petroleum source rock on the UK Continental Shelf (upper Permian, offshore Yorkshire)

Mirosław Słowakiewicz, Jon Gluyas, Adam Kowalski, Thomas Edwards, Samuel Słama, Mike Mawson, Maurice E. Tucker, Paul Scovell, Israel Polonio

Please cite this article as: Słowakiewicz, Mirosł., Gluyas, J., Kowalski, A., Edwards, T., Słama, S., Mawson, M., Tucker, M.E., Scovell, P., Polonio, I., A new and working petroleum source rock on the UK Continental Shelf (upper Permian, offshore Yorkshire), *Marine and Petroleum Geology* (2020), doi: https://doi.org/10.1016/j.marpetgeo.2020.104605.

This is a PDF file of an article that has undergone enhancements after acceptance, such as the addition of a cover page and metadata, and formatting for readability, but it is not yet the definitive version of record. This version will undergo additional copyediting, typesetting and review before it is published in its final form, but we are providing this version to give early visibility of the article. Please note that, during the production process, errors may be discovered which could affect the content, and all legal disclaimers that apply to the journal pertain.

CRediT authorship contribution statement

M.S. designed the project, analysed the data and wrote the manuscript. This study is partly based on S.S.'s BSc thesis (Słama, 2019) supervised by M.S., which provided some biomarker analyses. J.G. provided oil samples. A.K. performed the GC-FID and GC-MS. T.E. and P.S. provided seismic and geological data and oil samples. J.G., S.S., M.M., M.E.T., I.P. contributed to writing the article. All authors approved the manuscript.

1 **A new and working petroleum source rock on the UK Continental Shelf (Upper**

2 **Permian, offshore Yorkshire)**

3

4 Mirosław Słowakiewicz[1,2*], Jon Gluyas[3], Adam Kowalski[4], Thomas Edwards[5], Samuel Słama[1], Mike

5 Mawson[6], Maurice E. Tucker[7], Paul Scovell[8], Israel Polonio[9]

6

7 [1]Faculty of Geology, University of Warsaw, ul. Żwirki i Wigury 93, 02-089 Warsaw, Poland

8 [2]Kazan Federal University, Kremlovskaya 18, 420008 Kazan, Russia

9 [3]Department of Earth Sciences, Durham University, Durham, DH1 3LE, UK

10 [4]Faculty of Geology, Geophysics an Environmental Protection, AGH University of Science of Technology, Al.

11 Mickiewicza 30, 30-059 Kraków, Poland

12 [5]Israel Chemicals Ltd UK, Boulby Mine, Loftus, Saltburn, TS13 4UZ, UK

13 [6]24 Kenton House, Hartburn, Stockton-on-Tees, Teesside TS18 5EX, UK

14 [7]School of Earth Sciences, University of Bristol, Bristol, BS8 1RJ, UK

15 [8]Boulby Underground Laboratory, Boulby Mine, Loftus, Saltburn-by-the-Sea, Cleveland, TS13 4UZ, UK

16 [9]Lundin Norway AS, Strandveien 4, P.O. Box 247, N-1326 Lysaker, Norway

17

18 [*]corresponding author: m.slowakiewicz@gmail.com; m.slowakiewicz@uw.edu.pl

19

20 **Abstract**

21 We report on the discovery of oil from the Boulby Mine and its likely productive source rock

22 from Yorkshire in NE England, located to the west (<30 km) of the newly licenced petroleum

23 exploration areas in the vicinity of the Mid-North Sea High. Oil samples from the mine have

24 likely been generated from Zechstein Group Kirkham Abbey Formation (KAF) sapropelic

25 carbonate rock as indicated by aliphatic and aromatic hydrocarbon biomarkers. Other

26 potential source rocks of Carboniferous (Westphalian, Namurian, Viséan coals and

27 mudrocks) and Jurassic (the Jet Rock, Bituminous Shales, Kimmeridge Clay Formation) age

28 are ruled out on the basis of organic geochemical data. Boulby oil was generated in the peak-

29 to-late oil-window and it is characterised by the high abundance of C_{32} and C_{34} homohopanes,

30 slight even-over-odd predominance (EOP) of C_{20-25} *n*-alkanes indicating restricted carbonate-

31 evaporite depositional conditions, and C_{29} ethyl-diacholestane 20S likely implying a clay-rich

32 source rock. The structural framework and tectonic history of the Permian strata reveal the

33 presence of several fault systems which served as conduits for migrating petroleum. Similar

34 Zechstein-sourced oil is known from Poland and Germany, but the occurrence at Boulby is

35 the first positive identification of oil derived from Zechstein source rock in the North Sea

36 area. The Boulby oil is reservoired in Zechstein 3 (Z3) Brotherton Formation dolomite and

37 sealed by Z3 evaporite rocks. The proven oil occurrence at Boulby has significant

38 implications in terms of reducing the risk of a lack of oil mature source rock for acreage

39 offered in the neighbouring North Sea during the UK's 30th and 31st licencing rounds.

40 **Keywords**: seeping oil, source rock, Boulby Mine, Yorkshire, Zechstein, Late Permian

41

1. Introduction

43   The Boulby Mine opened in North Yorkshire, England, in 1973 (Woods, 1979, 1973)

44 for the mining of halite, polyhalite and sylvite from strata of Late Permian (Zechstein cycle 2

45 [EZ2] and 3 [EZ3]) age. The sylvite was originally identified in a prospect drilled for oil by

46 the D'Arcy Exploration Company in 1939 at Aislaby on the Eskdale Anticline. Well Eskdale

47 2 (Fig. 1), drilled a few km south of the present location of the mine, proved potash-bearing

48 minerals within three cycles of the Zechstein evaporite succession (EZ2, EZ3 and EZ4).

49   The mine workings reach a depth of 1300 m below sea level and extend ~8 km

50 towards and under the North Sea. The Boulby Mine is located in the Mesozoic Cleveland

51 Basin of northeast England (Fig. 1), which is the onshore development of the Sole Pit Trough.

52 It occurs on the margin of the Southern Permian Basin (SPB) of northwestern Europe, which

53 later became the North Sea Basin, containing thick sedimentary (sandstone-carbonate-

54 evaporite) sequences (Glennie and Underhill, 1998).
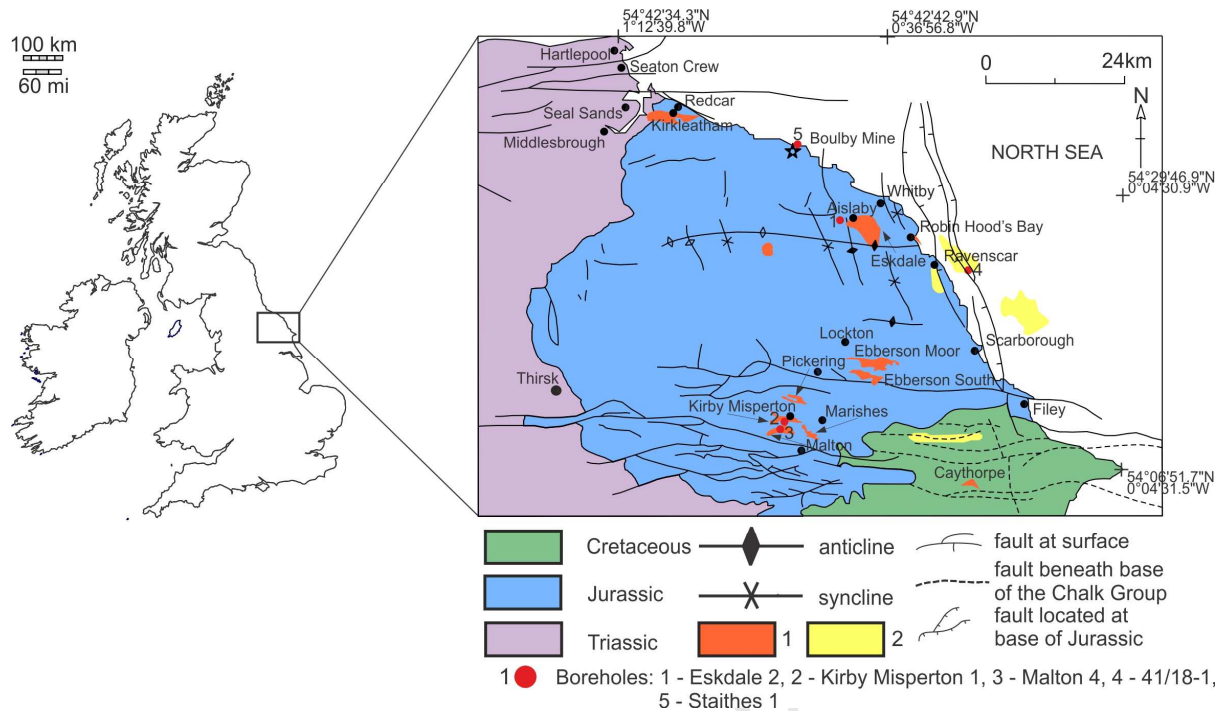
Fig. 1. Map of the Cleveland Basin and its major structural features indicating the position of the Boulby Mine (after Powell, 2010). The West Newton location is not shown and is ~113 km south of Boulby. 1 – gas fields; 2 – undeveloped gas discoveries (after Haarhoff et al., 2018).

In 2011, through fractures encountered during mining operations in a salt roadway and from an exploratory horizontal borehole drilled through the salt, a brine, oil and methane gas influx occurred. The origin of this seeping oil had been linked to the Carboniferous Coal Measures and terrigenous organic matter (OM) type (Davison, 2009). In the vicinity of the Boulby Mine, there are several gas fields (e.g., Eskdale, Lockton [now called Ebberson Moor], Malton, Marishes and Pickering; see Fig. 1, and the recent discovery at West Newton located ~113 km south of Boulby) hosted by Zechstein dolomites of the Kirkham Abbey (KAF) and Brotherton formations (EZ2 and EZ3, respectively; Fig. 2). Productive tests were reported from Namurian strata in the Kirby Misperton Field and from Rotliegend sandstone in the Caythorpe Field (also producing from the KAF) (Fig. 1). There have also been oil shows in a number of discoveries offshore of the Cleveland Basin (Quadrant 41), including well 41/18-1, just offshore of Robin Hood's Bay, and in KAF and Brotherton Formation carbonate rocks in the Teesside area close to the northern margin of the Cleveland Basin, including wells at Hartlepool and Seaton Carew (Smith and Francis, 1967 and references therein), as well as gas production at Kirkleatham (Fig. 1). It has long been assumed that the gas was generated from coal in the Upper Carboniferous interval. The Namurian source rock

76 present in the East Midlands and Liverpool Bay oil provinces has not been shown to be oil-

77 prone in the North Yorkshire area (Andrews, 2013). Other potential candidate source rocks

78 for the oil at Boulby Mine are Jurassic mudrock of the Lower Jurassic Jet Rock and

79 Bituminous Shales and the Upper Jurassic Kimmeridge Clay Formation (KCF). Some oil

80 seepage is known from septarian concretions within the Toarcian Jet Rock bituminous shale

81 exposed on the coast above the mine (Fig. 3), but shale is only marginally mature (Kent,

82 1980; Rawson and Wright, 1995, 2018). Further south along the coast the KCF is present but

83 thermally immature for petroleum. Boulby Mine is a considerable distance away (400 km)

84 from the Tail End Graben in the Central North Sea where the KCF is mature for petroleum

85 (Glennie et al., 2003).

86   To explore this conundrum and to test whether the Boulby oil was derived from

87 Carboniferous, Jurassic or a different source-rock we have recently collected four seeping oil

88 samples in a newly-opened part in the mine (2000 West Salt). Our new data include broader

89 organic geochemical analyses of Boulby oil allowing a detailed determination of the OM

90 source for the hydrocarbons, as well as the depositional conditions. We have quantified a

91 suite of biomarker signatures characteristic of past redox conditions, including homohopane

92 ratios, complemented by hopane and sterane distributions indicative of changes in OM source.

93 These, as well as geological and tectonic interpretations, are used to refine the origin of the

94 Boulby oil. These findings open a new window to petroleum exploration in the North Sea,

95 particularly in terms of defining several new pods of active source rock.

96

97
98
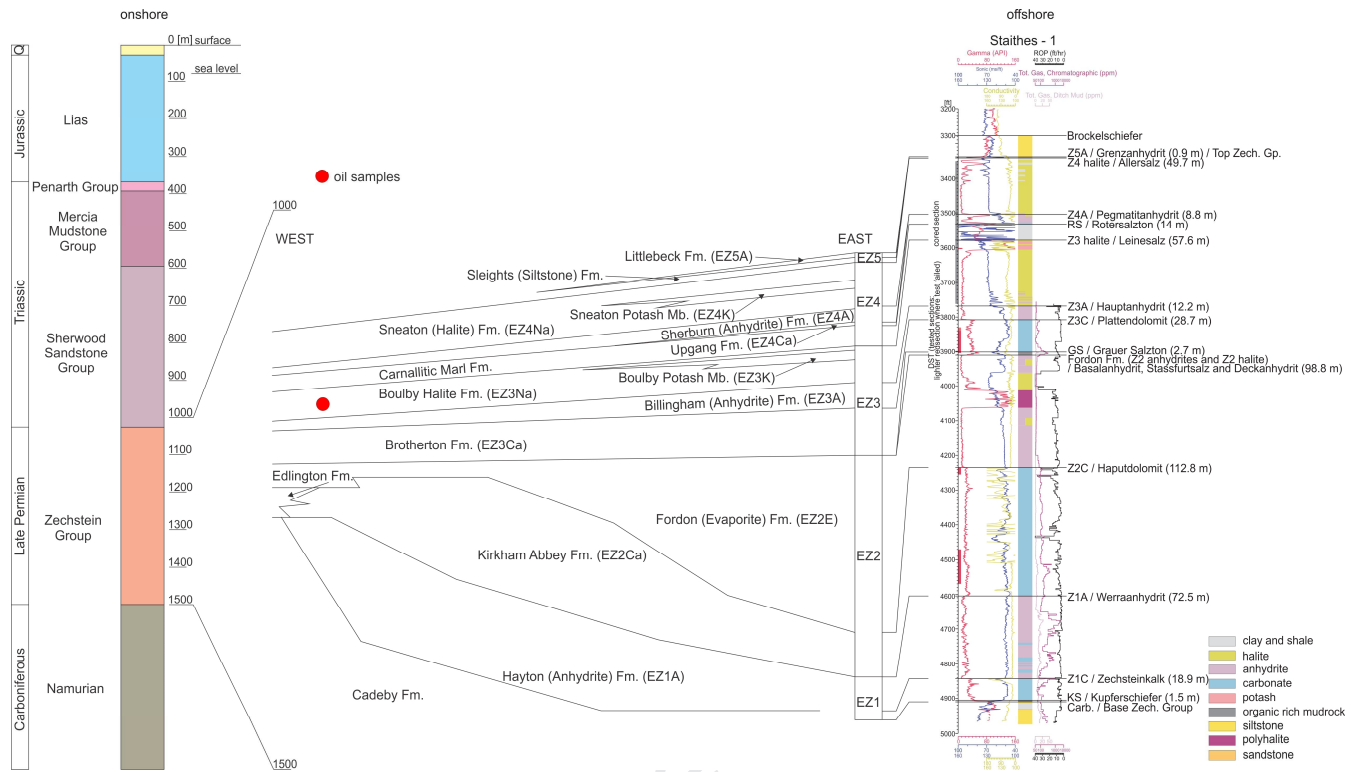
Fig. 2. Onshore (from the Boulby Mine) and offshore (well Staithes 1) stratigraphic correlation of the English Zechstein in NE Yorkshire (this paper and after Smith et al., 1986). Note the Chalk Group is absent in the Boulby area. EZ1-5 – English Zechstein cycles 1-5; Carb. – Carboniferous; Zech. Gp. – Zechstein Group.

102

Fig. 3. Oil seeping from a 'whalestone' concretion in Liassic bituminous mudstone at Port Mulgrave (photo courtesy of Jack Lee).

106

107

108

2. Geological setting

2.1. Stratigraphy

North Yorkshire and Cleveland Basin lithostratigraphy, modified after Kent (1980), is shown in Figure 2. The oldest rocks are mudstone and siltstone with carbonate beds (Lower Carboniferous, Craven Group, >760 m thick, comprising Bowland Shale Formation and Shale Limestone Unit), sandstone, mudstone and siltstone (Namurian Millstone Grit Group, 730 m thick) and a thick succession of Upper Carboniferous mudstone/siltstone with coal (Westphalian Coal Measures Group, 620 m thick, absent in the Boulby Mine area). Permian strata are Upper Rotliegend (Guadalupian) Yellow Sands (aeolian sandstone and breccia, although absent in the Boulby Mine area) and Zechstein evaporite and carbonate rocks (~400 m thick). The Zechstein Group consists of five cycles (EZ1-EZ5) containing thick halite and carbonate and thin anhydrite and potash units. Carbonate rocks comprise dolomites of the KAF (EZ2Ca = Hauptdolomit in the Southern North Sea, western SPB) and Brotherton Formation (EZ3Ca = Plattendolomit in western SPB). They are sealed by halite and anhydrite beds of the EZ1, EZ2 and EZ3 cycles. Zechstein rocks are overlain by the Triassic Sherwood Sandstone (350 m thick), Mercia Mudstone (320 m thick) and Penarth groups (20 m thick). Lower Jurassic (Lias Group shale, 435 m thick), Middle Jurassic and Upper Jurassic strata, which crop out extensively along the southern side of the Cleveland Basin and Quaternary sediments complete the stratigraphy in the Boulby area.

2.2. Basin development

Since the Late Palaeozoic the Cleveland Basin area has undergone two major phases of basin development (Holliday, 1999). The first of these was rapid burial in the Carboniferous terminated by the Variscan Orogeny at the end of the Carboniferous (Corfield et al., 1996). The second, more recent event developed throughout much of the Mesozoic, terminating with uplift in the Paleogene (Kent, 1980; Imber et al., 2014).

The Carboniferous interval in the Cleveland Basin is known only from a few boreholes drilled onshore for petroleum exploration (Malton 4, Kirby Misperton 1; Słowakiewicz et al., 2015), waste chemical disposal (Seal Sands near Hartlepool; Johnson et al., 2011; Andrews, 2013), and offshore for petroleum exploration in Quadrant 41 (Besly, 1998). The oldest strata penetrated belong to the Fell Sandstone Formation (Arundian = Viséan). The Fell

141   Sandstone Formation is known from outcrop further north in Northumberland to have been
142   deposited in a high-energy fluvial system. It is overlain by a shale-dominated interval with
143   subordinate sandstones and limestones deposited in paralic to shallow-marine conditions
144   during a syn-rift episode (Fraser and Gawthorpe, 1990). Post-rift sediments are also largely
145   paralic but with substantially more sandstone (Millstone Grit and Coal Measures groups).
146   The maximum thickness of the Carboniferous interval is in excess of 3000 m (Imber et al.,
147   2014). By the end of the Carboniferous the area of the current Cleveland Basin was
148   undergoing inversion resulting from the Variscan Orogeny and this resulted in the removal of
149   the Coal Measures Group over large areas so that the Permian strata commonly overstep
150   Namurian and Dinantian rocks. Uplift and erosion of the Cleveland area lasted until the
151   Early Permian when a second phase of rifting began.

152   By the Early Permian the area was within the single Pangea supercontinent and, although
153   subsidence had lowered the basin surface below contemporaneous sea level, the area was not
154   inundated. A land-locked basin developed with sedimentation occurring under aeolian,
155   sabkha and ephemeral fluvial conditions to form the Yellow Sands Formation. This sandstone
156   has been comprehensively described immediately north of the Cleveland Basin (but is absent
157   in the Boulby Mine area) in County Durham where it crops out and where quarrying has
158   afforded good exposure. The Yellow Sands Formation constitutes a series of NE-SW
159   trending sand ridges up to 60 m high and 1.5 to 3.5 km wide, separated by areas up to 2 km
160   wide that lack sand (Steele, 1983).

161   Sandstone deposition ended when the barrier to the Tethyan Ocean to the south east was
162   breeched and the seaway to Panthalassa in the north opened up so that what had been a sub-
163   sea-level basin dominated by deposition of terrestrial sediments became the Zechstein Sea.

164   The Late Permian was mostly a period of regional subsidence allowing up to many 100s
165   m of carbonate and evaporite units of the Zechstein Group to be deposited (Smith, 1989;
166   Taylor, 1998). These sediments form broadly off-lapping packages of carbonate and
167   anhydrite, with one major phase of basin-filling halite (EZ2E, Fordon Formation evaporite =
168   Stassfurt evaporites in the SPB). There is evidence in County Durham for some
169   synsedimentary fault movements which controlled deposition of the EZ1Ca reef (Ford
170   Formation = Zechstein Limestone in the SPB, Daniels et al., 2020).

171   The Mesozoic cover sequence in the area comprises Triassic and Jurassic sedimentary
172   rocks, the youngest being Middle Jurassic at the surface across the North Yorkshire hills.
173   Younger, Upper Jurassic rocks are exposed along the southern margin of the Cleveland Basin

174 (Powell, 2010), and, together with Cretaceous strata, crop out immediately south of the area

175 of interest and would in the past have been part of the sedimentary cover at Boulby before

176 Paleogene inversion. According to Holliday (1999) there was probably a thick succession of

177 Chalk Group and Paleogene sediments present prior to Paleogene uplift and erosion.

178   The Triassic succession, divisible into a lower Sherwood Sandstone Group, an upper

179 Mercia Mudstone Group and the Penarth Group, is still present in the subsurface. The likely

180 original thicknesses of these strata are up to 685 m (350 m, 320 m, 15 m, respectively; Kent,

181 1980). The Sherwood Sandstone Group was predominantly deposited by braided fluvial

182 systems and the overlying Mercia Mudstone Group sediments accumulated as playa lake

183 deposits.

184   The Lower Jurassic strata of the Lias Group are up to 435 m thick and dominated by

185 mudstone with subordinate sandstone and ironstone (Powell, 2010). The Redcar Mudstone

186 Formation (256 m) occurs at the base and includes calcitic, siliceous and pyritic/ironstone

187 marine shales. The shales are overlain by the Staithes Sandstone Formation (25 m) deposited

188 below wave-base in marine conditions as storm beds (van Buchem and Knox, 1998). The

189 youngest section of the Lower Jurassic Lias Group comprises the Whitby Mudstone

190 Formation (107 m thick), which, near the base, in the Mulgrave Shale member, contains

191 organic-rich mudrocks of the 8.5 m thick Jet Rock (equivalent to the Schistes Carton of the

192 Paris Basin) and overlying 23 m of thick Bituminous Shales (Rawson and Wright, 1995,

193 2018).

194   The Middle Jurassic strata are the youngest rocks exposed in the vicinity of the Boulby

195 Mine; they also crop out extensively in the Cleveland Basin and most comprise non-marine

196 siliciclastics with minor coal of the up to 240 m thick Ravenscar Group (Powell, 2010).

197 Deposition occurred in a range of paralic sub-environments, shallow-marine to delta-top.

198 Younger Jurassic strata crop out towards the southern margin of the basin, ~30 km to the

199 south of the Boulby Mine, and include the Oxford Clay, carbonate rock of the Corallian

200 Group and, at the top of the preserved succession, the ~300 m thick KCF mudrock.

201

202 *2.3. Inversion*

203   The area of the Cleveland Basin has undergone two phases of inversion since the

204 beginning of the Late Palaeozoic (Kent, 1980; Chadwick et al., 1993; Holliday, 1999). The

205 Variscan Orogeny caused a regional phase of uplift at the end of the Carboniferous as the

206 supercontinent Pangea came into existence. Uplift was substantial, causing on the order of

207 1.5 km of erosion as a minimum in the Cleveland area (Kent, 1980) and, offshore in Quadrant

208 42 (80 km east of Boulby), Lower Permian sediments overlie Devonian strata (Underhill,

209 2003). The Zechstein Group overlies Devonian rocks also in parts of Quadrant 38 (Taylor,

210 1998). This phase of uplift resulted in the removal of Coal Measures as a potential source

211 rock, as well as the uplift of older source rocks, i.e., the Carboniferous Bowland Shale

212 Formation mudrock.

213 A second phase of uplift occurred in the Late Cretaceous. In the Cleveland Basin an

214 estimated 1 to 1.5 km of Upper Cretaceous to Upper Jurassic sediment was stripped off (Kent,

215 1980; Imber et al., 2014), leaving the Middle Jurassic paralic sediments as the youngest now

216 seen in the area.

217

218 *2.4. Candidate source rocks*

219 In this section an overview of potential source rocks for Boulby oil in the Cleveland

220 Basin is provided. These include Upper Jurassic KCF mudrock, Toarcian shale and coal,

221 Zechstein lagoonal facies, Carboniferous Coal Measures, as well as Namurian and Viséan

222 mudrocks.

223 *2.4.1. Kimmeridge Clay Formation (KCF)*

224 The organic richness of KCF mudrock (300 m thick) and the results of Rock-Eval

225 pyrolysis show that the average total organic carbon (TOC) values are 5-8 wt.%; the quality

226 of kerogen is excellent with respect to hydrocarbon generation, and the hydrogen index (HI)

227 ranges from 500 to 600 mg HC/g TOC. In some places where there is an immature-mature

228 transition the TOC and HI values reach 32 wt.% and 1200 mg/g TOC, respectively;

229 sapropelic marine kerogen type II predominates (Scotchman, 1991). The $\delta^{13}C$ values of

230 saturated and aromatic bitumen fractions range from -32 to -25 ‰ (Bailey et al., 1990;

231 Cooper et al., 1995; van Kaam-Peters et al., 1997; Gautier, 2005).

232 The features of KCF source rock are a significant enrichment of C_{33-35} homohopanes (de

233 Leeuw and Sinninghe Damsté, 1990), a high abundance of 28,30-bisnorhopane (Grantham et

234 al., 1980; Peters et al., 1989), a dominance of C_{27} and C_{29} steranes (Mackenzie et al., 1983;

235 Huc et al., 1985), and the presence of isorenieratene derivatives (van Kaam-Peters et al.,

236 1997; Sinninghe Damsté et al., 2001).

237 *2.4.2. Lower Jurassic mudrocks of the Jet Rock and Bituminous Shales*

238   Lower and Middle Jurassic coals and shales are believed to contribute locally as
239 petroleum sources (Husmo et al., 2002). Jet Rock and Bituminous Shales form part of the
240 Mulgrave Shale Member at the base of the Whitby Mudstone Formation. The Jet Rock's
241 equivalents in the Paris Basin (Schistes Carton) and Germany (Posidonienschiefer) are
242 petroleum source rocks. The TOC content in Toarcian shale of Runswick Bay varies from 2.5
243 to 18.9 wt.%; HI ranges from 500 to 700 mg HC/g TOC, and kerogen type II is predominant
244 (Song, 2015; Song et al., 2015). Vitrinite reflectance values are between 0.6 and 0.7 %R_o
245 (Song, 2015; Song et al., 2015), indicating the early oil generation window. The $\delta^{13}C$ values
246 of OM in the shale vary from -27.3 to -25 ‰ (Bailey et al., 1990).

247   *2.4.3. Zechstein Group carbonate rocks*

248   Kirkham Abbey Formation (KAF) carbonate rocks (Zechstein cycle 2, EZ2) in the
249 Cleveland Basin area, which are sealed at the top and bottom by the Fordon Formation and
250 Hayton Anhydrite evaporites, respectively, chiefly consist of ramp to slope facies (lagoonal,
251 oolitic, turbiditic, pelagic, slump and debrite carbonate rocks), which extend landwards and
252 interfinger with siliciclastic lagoonal-evaporitic facies of the Edlington Formation (Smith,
253 1989; Taylor, 1998). Clay- and microbial- rich lagoonal dolomites are, in addition to lower
254 slope facies and chicken-wire anhydrites, regarded as source rocks for Zechstein oil in the
255 central and eastern SPB (Słowakiewicz et al., 2018). Lagoonal carbonate facies in the
256 Yorkshire area have TOC <2 wt.% and thickness ~25-35 m (Słowakiewicz et al., 2016). In
257 addition, thinly-laminated basinal calcareous mudstone, named Stinkschiefer in the SPB,
258 commonly regarded as a source rock for hydrocarbons, has previously been ruled out by
259 Słowakiewicz and Gąsiewicz (2013) as an effective source rock. Furthermore, Zechstein
260 cycle 3 (EZ3) Plattendolomit (= Brotherton Formation) representing ramp facies are only
261 regarded as good reservoir rocks for petroleum in the North Sea (e.g., Wissey field located in
262 the southern North Sea, Duguid and Underhill, 2010), although bituminous organic-rich
263 limey mudstone of the Grauer Salzton Formation (the lowermost unit of the Plattendolomit)
264 (Duguid and Underhill, 2010) might serve as a potential source rock. In addition, Zechstein
265 lagoonal carbonates with anhydrite units may also be potential source rocks, with the OM
266 derived from former microbial mats with clay.

267   *2.4.4. Carboniferous Coal Measures Group*

268   The Westphalian Coal Measures Group represents cyclic fluvio-deltaic sedimentation in a
269 lower delta-plain environment at times when the influx of sand was at a minimum (Fraser and

270   Gawthorpe, 1990; Burgess and Gayer, 2000). The majority of Westphalian sandstone

271   reservoirs are currently producing gas, which is sourced from Coal Measures with a possible

272   contribution from Namurian basinal shales (Kombrink et al., 2010). Westphalian coal source

273   rocks are largely absent from the Cleveland Basin (Haarhoff et al., 2018) due to Variscan

274   uplift over wide areas prior to deposition of Permian sediments.

275   *2.4.5. Namurian and Dinantian source rocks*

276   Lower Carboniferous and Namurian source rocks are represented by black shale formed

277   in marine deep-water basins and coal developed on terrigenous to marginal-marine delta

278   plains (Fraser and Gawthorpe, 1990). Basinal shale alternating with carbonate beds was

279   deposited on the slope of carbonate platforms and in the basinal areas. After carbonate

280   sedimentation ceased (Namurian-Viséan transition) black shale was deposited across

281   carbonate platforms (e.g., Bowland Shale Formation on the Derbyshire Block). In the basinal

282   areas, black shale deposition continued from the Viséan into the Namurian (Pletsch et al.,

283   2010).

284   Petroleum has been found in fractured Viséan shelf carbonates sourced by Namurian

285   basinal shale at a number of locations in Derbyshire (Fraser and Gawthorpe, 1990; DECC,

286   2013). Highly mature Hardstoft oil (located south of Chesterfield, in eastern Derbyshire) is

287   sourced from Viséan calcareous shale (Craig et al., 2015, and our unpublished biomarker

288   data). Namurian and lower Westphalian (Langsettian) sandstone reservoirs host several oil

289   and gas fields in the East Midlands, Gainsborough Trough and Yorkshire. In all cases the

290   source rock is gas-prone Namurian basinal shale and Westphalian Coal Measures (Kombrink

291   et al., 2010).

292   The Namurian Bowland Shale Formation of the Cleveland Basin has been identified as

293   having substantial unconventional hydrocarbon resource potential (Andrews, 2013; Haarhoff

294   et al., 2018). TOC of Bowland Shale Formation mudrock varies from 1.3 to 9.1 wt.%; the

295   dominant kerogen is a gas-prone humic terrigenous type III, and the Carboniferous section is

296   mature for gas generation in the Cleveland Basin (Hughes et al., 2018) and further south in

297   the Pennine Basin (Gross et al., 2015).

298   In addition, in the Great Limestone Member (Namurian) Creaney et al. (1980) reported

299   the presence of bitumen characterised by the predominance of low molecular weight *n*-

300   alkanes in calcite veins. The Great Limestone Member belongs to the Yoredale Group, which

301   comprises repeated sequences of limestone, shale, sandstone and coal. The average thickness

302 of these cycles is ~30 m (Chadwick et al., 1993), of which dark limestone, shale and coal

303 might serve as a potential source rock for petroleum. Similarly, Edale oil (located southwest

304 of Boulby, in northern Derbyshire) is sourced from the Edale Shale Group mudrock (=

305 Bowland Shale Formation) of the lowermost Namurian (Fraser and Gawthorpe, 1990; Gluyas

306 and Bowman, 1997). Also, in the Midland Valley of Scotland, Viséan Strathclyde Group oil

307 shale is a rich source rock for petroleum (Underhill et al., 2008).

308 *2.5. Distribution and perception of thermal maturity*

309 Thermal maturity development in the Cleveland Basin is still poorly understood.

310 According to Barnard and Cooper (1983) Carboniferous Coal Measures Group sediments

311 have thermal maturity >2 % on the vitrinite reflectance scale (R_o), whereas Middle and Upper

312 Jurassic rocks have R_o values from 0.3 % in southern part of the Cleveland Basin to 0.8 % in

313 the Boulby area, also suggesting greater burial in the latter. Curiously, in the Malton area (Fig.

314 1) R_o is ~0.3 % in Jurassic rocks, but 20 km farther north at Lockton, R_o values increase (R_o

315 0.5-0.6 %), which might imply the influence of fault-related hydrothermal higher heat flow

316 (Barnard and Cooper, 1983; Imber et al., 2014). Based on the illite-smectite assemblage

317 Kemp et al. (2005) suggested burial depths of 4 km and a geothermal gradient of 25-30

318 ^{o}C/km for Lias shale. In addition, the Toarcian Whitby Mudstone Formation is in the early oil

319 window (French et al., 2014), but the Carboniferous Bowland Shale-Hodder Mudstone shales

320 are thermally mature for gas (Haarhoff et al., 2018). Higher thermal maturity (R_o ~0.8-0.9 %)

321 has also been noted in Lockton 2a KAF limestone slope facies, revealed by negative $\delta^{18}O$

322 values (-2 to -14 ‰), the presence of saddle dolomite and increased abundance of tricyclic

323 and tetracyclic terpenoids (Słowakiewicz et al., 2016).

324

3. Materials and methods

3.1. Sample collection

327 Four crude-oil samples (one Boulby black oil [sample 1] and three light-brown Boulby oil

328 [samples 2-4] samples) dripping out of fractures in rock salt of the Boulby Halite Formation

329 (EZ3Na, Figs 2,4) from the roof of the Boulby Mine at workings (2000 West Salt) at a depth

330 of 1100 m subsurface were collected by hand into pre-furnaced glass jars. The glass jars were

331 sealed with pre-furnaced aluminium foil and stored at 4 °C.

332   In addition, comparisons are made in this paper to previously published and reported

333   herein biomarker data from fourteen samples of KAF dolomite lagoonal facies (onshore

334   equivalent of the Innes Carbonate Member of the NPB) of the Malton 4 well (Słowakiewicz

335   et al., 2016), and typical carbon isotopic values for saturated and aromatic fractions of

336   Jurassic, Permian and Devonian oil from the SPB and North Sea areas.

337   *3.2. 3D seismic data*

338   A 3D seismic survey was undertaken by ICL UK Ltd in 2011 as part of an ongoing

339   exploration programme for potash and polyhalite. The data reveal some interesting structural

340   features which correlate with both the locations of the oil samples collected in this study and

341   with previous instances of hydrocarbons in this specific area of the mine. Data for this

342   survey were acquired by CGG and processed by Fugro. Interpretation was carried out by a

343   combination of external contractors and on-site staff at the Boulby Mine.

344   *3.3. Density determination of Boulby oil samples*

345   Oil samples were analysed at 20 $^{\circ}$C for API gravity using an Anton-Paar DMA^{TM} 5000 M

346   density meter. A minimum of two replications were collected for each sample and the

347   average value was used.

348   *3.4. Extraction and biomarker analyses*

349   Approximately 120 mg of the crude-oil samples were subjected to a fractionation

350   procedure. Prior to this, asphaltenes were precipitated by adding 60 mL petroleum ether to (at

351   maximum) 100 mg of sample. Subsequently, the mixture was centrifuged at 1600 rpm for 10

352   min. The supernatant solution containing maltenes was collected and the solvent removed

353   through evaporation in a nitrogen atmosphere at 35 °C. Asphaltenes were then removed. The

354   residual maltenes (up to 100 mg) were separated into aliphatic and aromatic fractions on

355   silica gel (activated at 240 °C for 12 h), using a sequence of organic solvents of different

356   polarity (petroleum ether, toluene).

357   Aliquots (1 μL) of each fraction were analysed by gas chromatography (GC) using an

358   Agilent 7890A instrument, fitted with an on-column injector and an Agilent DB-5MS fused

359   silica capillary column (60 m × 0.25 mm; df = 0.10 μm) coated with 95 % dimethylarylene

360   siloxane and 5 % phenyl phase. Detection was achieved with flame ionization, with helium as

361   the carrier gas. The temperature programme consisted of four stages: 80 °C held for 1 min;

362   80°-120 °C at 20 °C min^{-1}; 120°-300 °C at 3 °C min^{-1}; and 300 °C with the temperature held

363   for 35 min. GC-mass spectrometry (MS) analyses were performed using an Agilent 5975C

364   mass selective detector (MSD) using the same column and temperature programme as for GC

365   analyses. The MS operated with an ion-source temperature at 230 °C, electron ionization at

366   70 eV, and a cycle time of 1 sec in the mass range from 45 to 600 Da. In the selected ion

367   mode (SIM) the dwell time of the operated MSD was set at 30 ms for each ion.

368   Measurements of aliphatic fractions were carried out on a Thermo Scientific TSQ Quantum

369   using parent-daughter-scans via multiple-reaction-monitoring (MRM), which overcomes

370   most of the interference caused by co-eluting peaks. The instrument was tuned to a resolution

371   of 0.7 mass units. The collision energy was 15 V with argon as the collision gas at a pressure

372   of 1.0 mTorr. The column used was a 60-m CP-Sil-5 CB-MS with an i.d. of 0.25 mm and a

373   film thickness 0.25 μm. The temperature programme was 50 °C held for 1 min; 50°-225 °C at

374   2 °C min^{-1}; 225°-300 °C at 20 °C min^{-1}; and 320 °C with the temperature held for 20 min.

375   Compounds were identified by comparison of retention times and mass spectra to the

376   literature. Peak ratio calculations for GC-FID and GC-MS were done from integrated

377   area:area and the biomarker ratios were computed as area:area as well. Individual compounds

378   were identified and quantified relative to internal standards (ortho-terphenyl).

379   *3.5. Stable carbon isotope analyses*

380   Stable carbon isotope ratios of the C_{15+} saturated and aromatic hydrocarbon fractions

381   were determined using a Finnigan Delta Plus MS. The $\delta^{13}C$ values are reported relative to the

382   Vienna Pee Dee Belemnite (VPDB) standard, and the analytical error, determined by using

383   co-injected standards, is ±0.2‰.

384

385
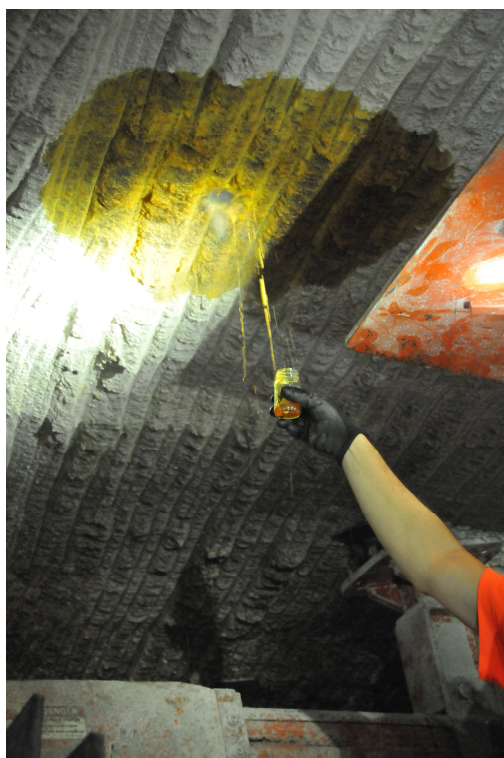
Fig. 4. Light-brown oil dripping out from fractures in rock salt of the Boulby Halite Formation from the roof of
the Boulby Mine at a depth of 1100 m (mine working 2000 West Salt).

388

4. Structural geology and organic geochemistry

4.1. Seeping oil density

Oil samples can be classified as light oils with API gravity ranging from 35.1^{o} to 42.2^{o}
(density 0.80984-0.84487 g/cm^3, Table 2), respectively, and cannot be linked directly to any
particular oil in the North Sea such as Chalk Group-, KCF-, Zechstein-, Carboniferous- or
Devonian-sourced oil (Evans et al., 2003).

4.2. Thermal maturity

Thermal maturity of Boulby oil and Malton 4 KAF samples (Table 1) is evaluated
based on the saturated and aromatic hydrocarbon ratios listed in Table 1. These ratios may be
affected by factors such as lithology and adsorption of OM on mineral surfaces, which may
affect maturation signatures and variations in biomarker distributions (Jiang et al., 1988;
Peters et al., 2005); thus interpretations should be based on a variety of maturity parameters.

The isoprenoid-based ratios Pr/n-C$_{17}$ and Ph/n-C$_{18}$ decrease with increasing thermal
stress due to the preferential release of n-alkanes during maturation, but they can be affected
by organofacies variation and biodegradation (Peters et al., 2005). These ratios show values

of 0.27 – 0.54 and 0.53–0.78 for Boulby oil samples and 0.17 – 0.58 and 0.21 – 0.58 for KAF
samples, respectively (Table 3a, Fig. 5).
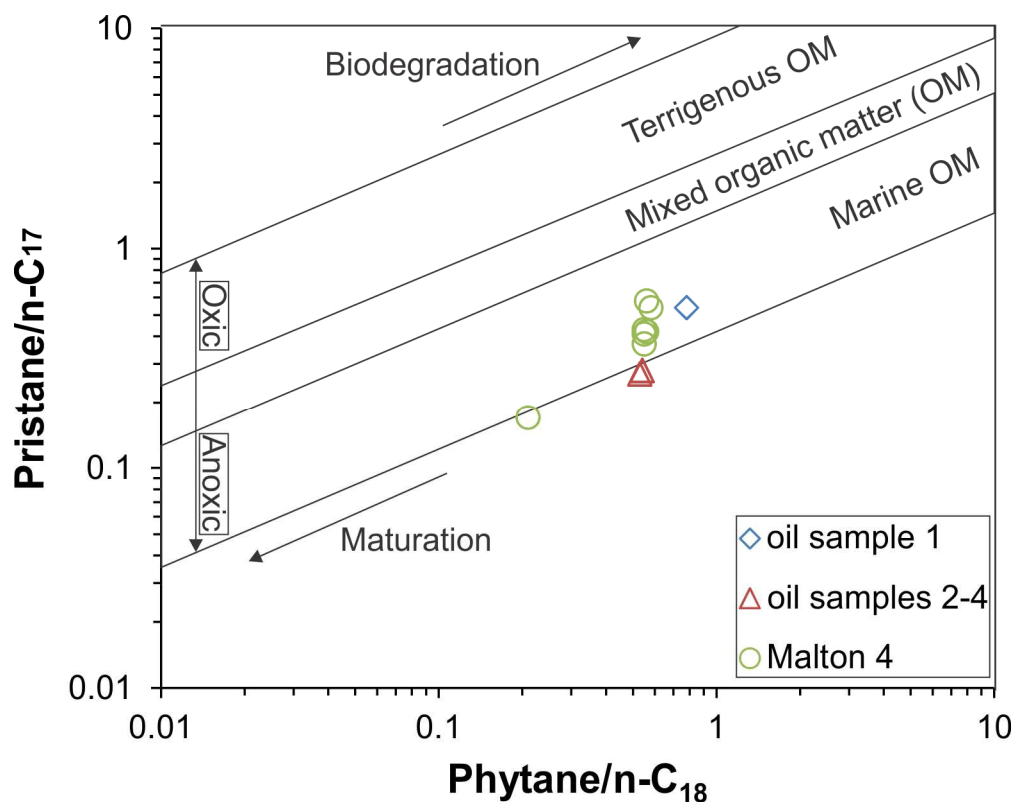
Fig. 5. Phytane to *n*-C_{18} alkane versus pristane to *n*-C_{17} alkane for Boulby oil (samples 1-4) and Malton 4 KAF
samples (graphical fields after Shanmugam, 1985).

The Ts/Tm ratio calculated from oil sample 1 is 0.41 and 0.52 – 0.71 from Malton 4
KAF samples (Table 1). The Ts/Tm ratio can also be affected by lithology; for example, in
carbonate settings Tm is preferentially generated (Peters et al., 2005). The M/H ratio in oil
sample 1 is 0.12 and in KAF samples is 0.03 – 0.13 (Table 1). The M/H ratio decreases with
thermal maturity from ~0.8 in immature bitumen to <0.15 in a mature source rock and oil to a
minimum of 0.05 (Mackenzie et al., 1980; Seifert and Moldowan, 1980). In Boulby oil
samples 2-4 the Ts/Tm and M/H ratios could not be determined due to high thermal maturity
or OM alteration after deposition.

The isomerisation equilibrium for ββ/(αα + ββ) and 20S/(20S + 20R) C_{29} steranes lies
between 0.67 – 0.71 and 0.52–0.57, respectively, and reaches equilibrium in the late and peak
oil window, respectively (Peters et al., 2005). Therefore, C_{29} steranes may have a limited
relevance in thermal maturity assessment (Walters et al., 2012). In oil sample 1 and KAF
samples, values for the ββ/(αα + ββ) ratio are 0.56 and 0.45 – 0.58, respectively, whereas the

424 20S/(20S + 20R) values are 0.52 in oil sample 1 and 0.46 – 0.57 in KAF samples, indicating

425 generation in the peak oil window (Table 1). The TA[I]/TA[I + II] ratio (Mackenzie et al.,

426 1981) increases with increasing maturity (Beach et al., 1989) and is indicative of mature and

427 late mature stages of oil generation (Peters et al., 2005). Values for TA[I]/TA[I + II] are 0.07

428 in oil sample 1 and 0.25 – 0.33 in KAF samples referring to the peak oil phase (Table 1).

429 Values for regular sterane and triaromatic steroid ratios in oil samples 2-4 could not be

430 determined due to the high thermal maturity of OM. As an alternative, a significant reduction

431 in the distribution of terpenoids would not only result from high thermal maturity or

432 diagenetic processes altering OM but also from the loss of more volatile hydrocarbons due to

433 evaporation during the dripping out from fractures.

434   The MDR value is 4.88 in oil sample 1 and 1.78 – 2.02 in KAF samples, respectively,

435 giving maturities in the range of 0.64 – 0.87 %Rm, whereas MPI 1 values in oil sample 1

436 (0.65) and oil samples 2-4 (1.3-1.4) give maturities in the range of 0.8-1.2 %Rc (Table 1) and

437 in KAF samples (0.68 – 0.77) are 0.8-0.9 %Rc (Table 1), indicating peak oil window

438 generation for oil sample 1 and KAF samples and late oil window generation for oil samples

439 2-4.

440   In summary, our data indicate that the Boulby oil samples were generated in the peak

441 to late oil window and Malton 4 KAF samples in the peak oil window.

442

443   *4.3. Molecular indicators of depositional environment*

444   4.3.1. Stable carbon isotopes

445   The carbon isotopic compositions of aliphatic and aromatic hydrocarbons of crude

446 oils are frequently used for correlation of oils (Fuex, 1977; Peters et al., 2005), to decipher

447 their marine or terrigenous origin (Sofer, 1984; Chung et al., 1992), or age (Andrusevich et

448 al., 1998). $\delta^{13}C$ values of the saturated fraction of the Boulby oil samples vary between -25.2

449 and -23.9 ‰, whereas the aromatic fraction has $\delta^{13}C$ values ranging from -24.4 to -22.6 ‰

450 (Fig. 6, Table 2). The canonical variable (CV, Sofer, 1984), which separates non-waxy

451 (marine) and waxy (non-marine) oil, varies between -3 and -0.5 (Table 2). All signatures

452 indicate that the source rock for the Boulby oil was deposited in a marine setting.

453      $\delta^{13}C$ values of the saturated and aromatic fractions of the Boulby oil are within the

454 range of Late Permian (Zechstein) oil in Europe (i.e. -31 to -24‰), although the values

455 between > -27.5 and -31‰ reported by Słowakiewicz et al. (2018) are of oils likely to have

456 been generated from a different source rock than the Zechstein (unpublished data). The

457 Boulby $\delta^{13}C$ values are different from those of the Late Jurassic (-31.5 to -27.8‰; Bailey et

458 al., 1990; Andrusevich et al., 2000; Peters et al., 2005; and this study) and Devonian (-35 to -

459 31‰; Bailey et al., 1990; Peters et al., 2005) oil in the North Sea (Fig. 6).
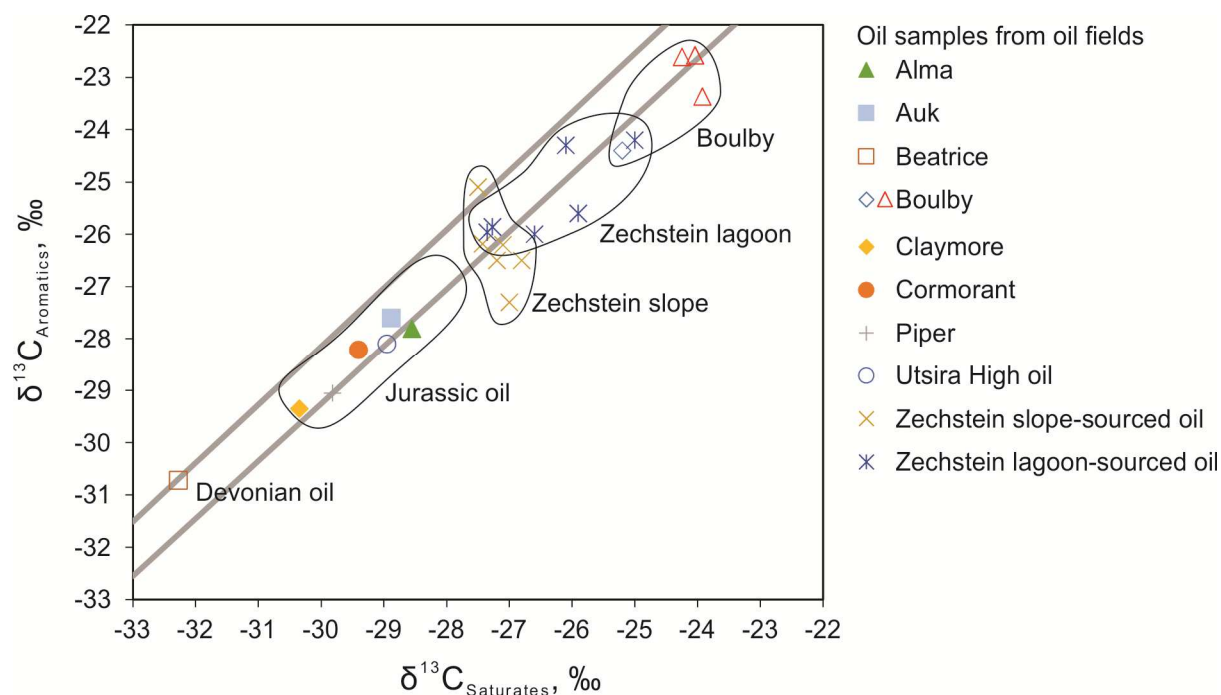
460

461 **Fig. 6.** Sofer's (1984) plot of $\delta^{13}C$ values for the saturated and aromatic fractions of various oil samples to

462 compare with the Boulby oil. Late Jurassic (Alma, Auk, Claymore, Cormorant, Piper, from Peters et al., 2005

463 and this study + Utsira High oil + data from Bailey et al., 1990), Zechstein (from Słowakiewicz et al., 2018),

464 and Devonian (Beatrice, from Peters et al., 2005) oils are given for comparison. Note that $\delta^{13}C$ values of

465 Devonian oil shows and bitumen range from -31.4 to -35‰ (see Bailey et al., 1990).

466

467 4.3.2. Water column characteristics

468 A suite of biomarkers was used to assess redox conditions and depositional

469 environment during formation of the source rocks for the Boulby oil, including the carbon

470 preference index (CPI), Pr/n-C_{17} versus Ph/n-C_{18}, even-over-odd predominance (EOP) of n-

471 alkanes, C_{31}-C_{35} homohopane distributions, and the homohopane index (HHI) expressed as

472 $C_{35}/(C_{31}-C_{35})$ and $C_{35}S/C_{34}S$ (Table 3a-c). Triterpenoids in Boulby oil samples 2-4 were

473 absent or significantly reduced due to high thermal maturity or OM degradation.

474 The CPI for all oil and KAF dolomite samples is close to 1 and 0.8 – 1, respectively,

475 and an EOP for the C_{20-25} n-alkanes is observed in oil samples (Fig. 7). An EOP in the range

476 of >n-C_{22} is typical of biomass deposited in restricted marine carbonate/evaporite facies

477 (Dembicki et al., 1976; Shen et al., 1980; Palacas et al., 1984; Ten Haven et al., 1985) and

478　can also be attributed to some specific bacteria or fungi (Han and Calvin, 1969; Jones, 1969;

479　Fisher et al., 1972).

480　　　　The values of Pr/n-C$_{17}$ versus Ph/n-C$_{18}$ in Figure 5 indicate primary accumulation of

481　marine OM under reducing conditions (Connan and Cassou, 1980; Palacas et al., 1984) for

482　the source rock of the Boulby oil. It should also be noted that short and long molecular

483　weight n-alkanes are reduced in some samples due to biodegradation (from non- to slight to

484　moderate biodegradation and presence of an unresolved complex mixture illustrated in Figure

485　7), thermal maturity (cracking), water washing or evaporative fractionation (Thompson, 1987,

486　1983; Holba et al., 1996; Akinlua et al., 2006). Homohopane distributions (Fig. 8) are used to

487　differentiate between oxic and reducing depositional environments, but the distributions can

488　be affected by thermal maturity and secondary alteration (Peters and Moldowan, 1991).

489　Slightly reducing (suboxic) depositional conditions are indicated by the HHI (0.14) and

490　C$_{35}$S/C$_{34}$S ratio (0.8) for Boulby oil. Slightly more anoxic depositional conditions are

491　deduced for the KAF dolomite samples (Table 3b).

492

493
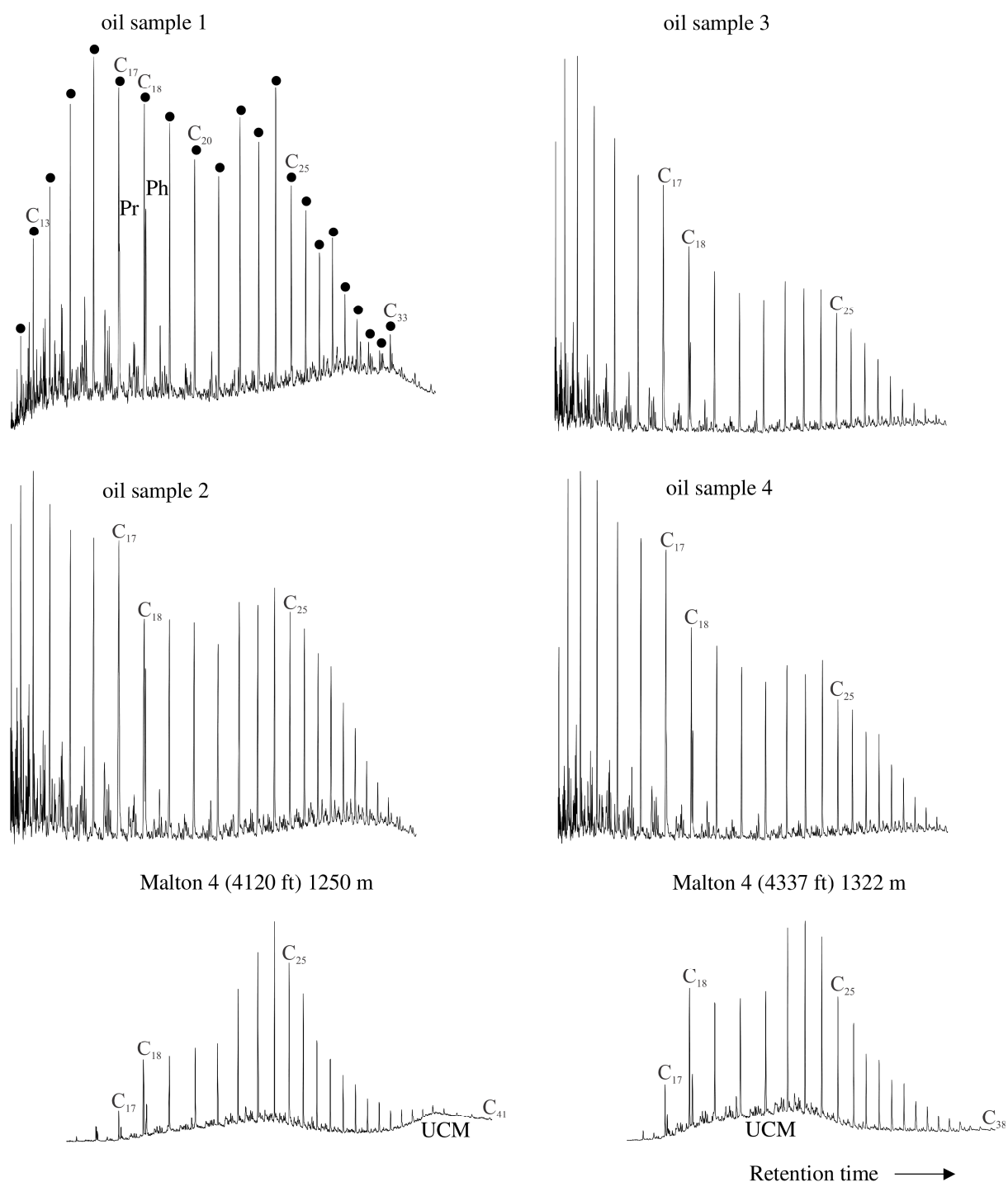
Fig. 7. Total ion current chromatograms of whole oil (Boulby oil samples 1 to 4) and selected Malton 4 dolomite (lagoonal facies) samples. Pr – pristane, Ph – phytane; black dots indicate *n*-alkanes. Note slight even-over-odd preference (EOP) for the C_{20-25} *n*-alkanes in Boulby oil samples. The EOP is not clear in Boulby oil sample 3. Note moderate biodegradation (classification after Wenger et al., 2002) with visible unresolved complex mixture (UCM for Malton 4 samples).

Boulby oil (particularly in oil sample 1) and KAF dolomite samples are characterized by the dominance of C_{30} 17$\alpha\beta$-hopane over lower or higher homologues and elevated relative

503 abundances of C_{32} and C_{34} hopanes (Boulby) and C_{32} and C_{35} hopanes (KAF) (Fig. 8, Table

504 3b), which are believed to indicate suboxic (high C_{32})/anoxic (high C_{34} or C_{35}) source-rock

505 depositional environments (Peters and Moldowan, 1991). The dominance of 17αβ-C_{32} over

506 C_{31} and C_{33} homologues and 17αβ-C_{34} over C_{33} and C_{35} homologues (Table 3b) indicates a

507 carbonate lagoonal and evaporitic environment source (Palacas et al., 1984; Jiamo et al.,

508 1986; Brassell et al., 1988; Waples and Machihara, 1991) or a depositional setting for oil

509 shale (Kara-Gülbay and Korkmaz, 2008). However, elevated 17αβ-C_{34} and C_{35} hopanes are

510 also characteristic for Late Permian (Zechstein) oil from south-central Germany derived from

511 a carbonate-evaporite source rock (Słowakiewicz et al., 2018).

512   Biomarkers for anaerobic phototrophic green sulphur bacteria provide strong evidence

513 of the redox state and water column stratification indicating photic zone euxinia (PZE) during

514 source rock deposition (Summons and Powell, 1986; Sinninghe Damsté et al., 1993).

515 Isorenieratene derivatives C_{18-21} 2,3,6-aryl isoprenoids are present in oil sample 1 and KAF

516 samples; in two KAF samples even isorenieratane has been detected (not shown). The

517 absence or low abundance of isorenieratene derivatives in the other oil samples is likely a

518 result of the thermal maturity effect (Requejo et al., 1992).

519

520
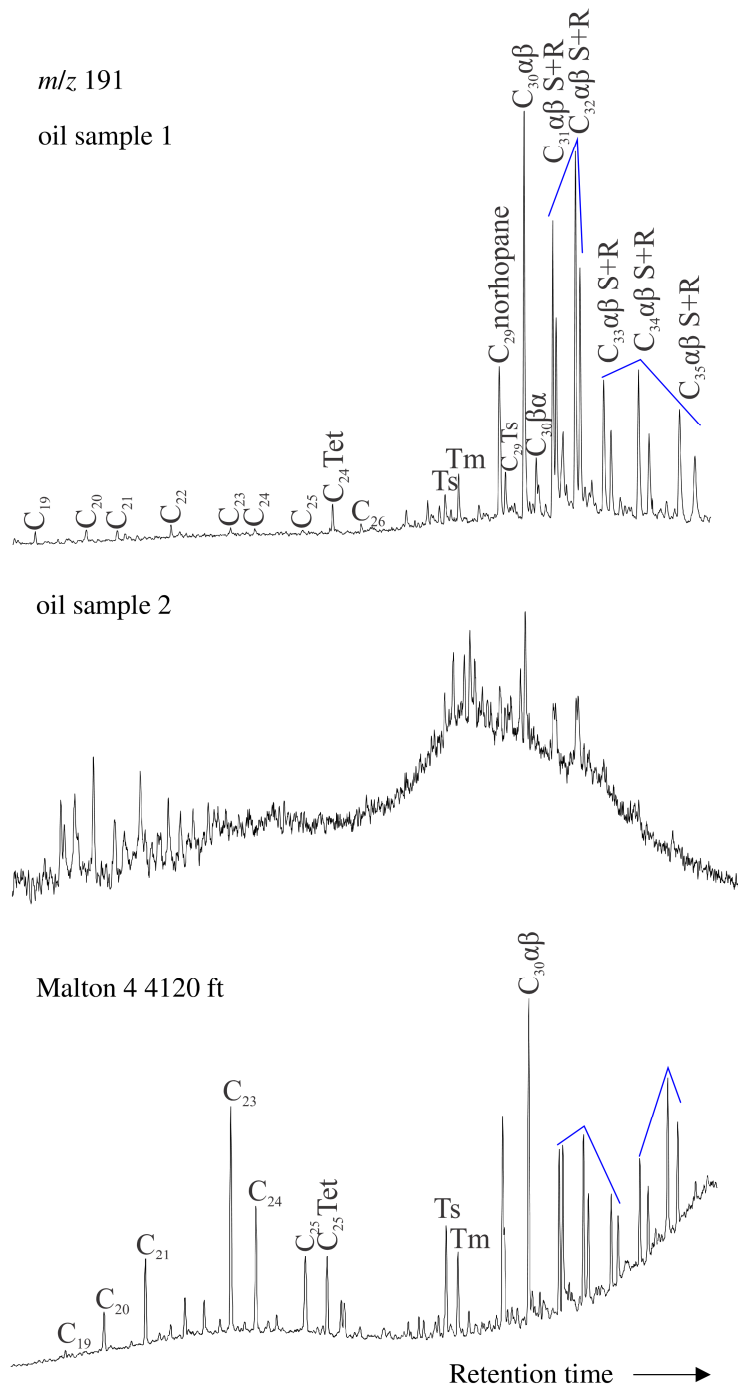
Fig. 8. Terpane mass chromatograms for Boulby oil samples and Malton 4 lagoonal facies have elevated C_{32}, C_{34} and C_{35} homohopanes indicating carbonate-evaporite source-rock depositional conditions. Some terpanes are absent in Boulby oil sample 2 due to high thermal maturity. Distribution of biomarkers in oil sample 2 is similar in oil samples 3 and 4.

4.3.3. Source of organic matter

The source rock for Boulby oil can be explored using $C_{35}S/C_{34}S$, the C_{29} $17\alpha\beta$-norhopane/C_{30} $17\alpha\beta$-hopane (C_{29}/H), C_{19}/C_{23} tricyclic terpane and diasterane/sterane ratios expressed as C_{27} or C_{29} $13\beta,17\alpha(H)$ (20S + 20R)/(C_{27} or $_{29}$ $5\alpha,14\alpha,17\alpha(H)$ 20S + 20R + $5\alpha,14\beta,17\beta(H)$ 20S + 20R).
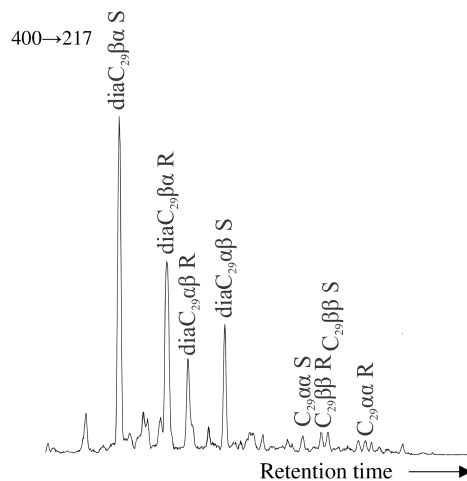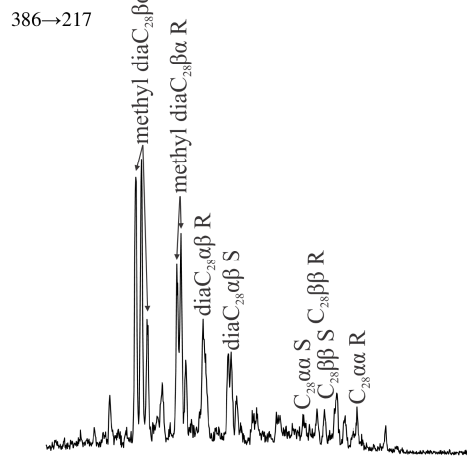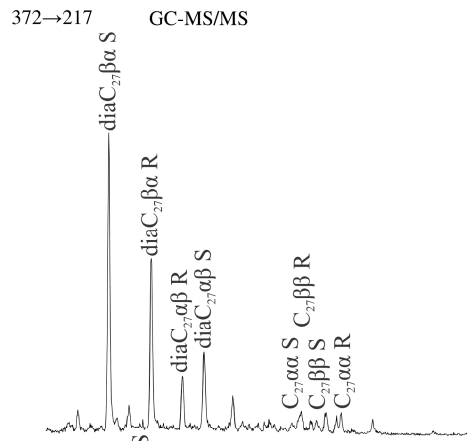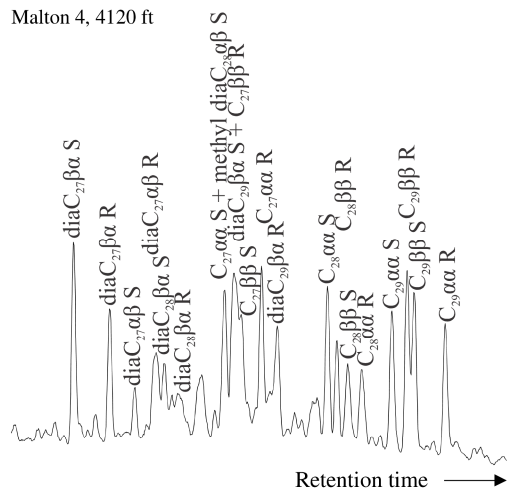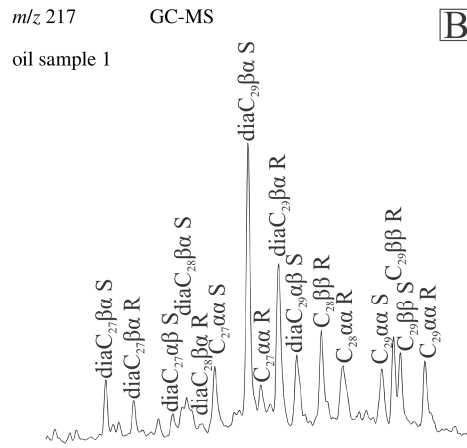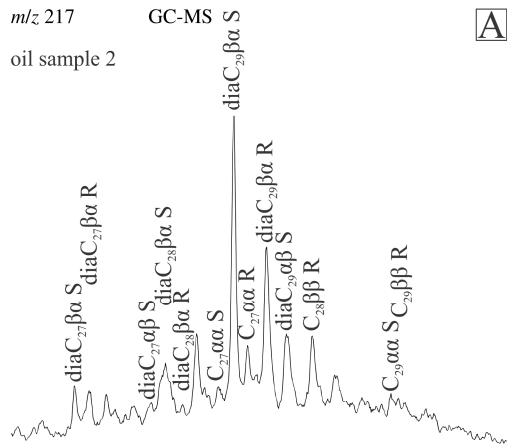
High C_{29}/H (>0.8) in oil is commonly reported as derived from anoxic carbonate or a marl source rock (Palacas et al., 1984; Clark and Philp, 1989). In oil sample 1 the C_{29}/H ratio is 0.27 and in KAF dolomite samples this ranges from 0.5 to 1.2 (mean 0.74) (Table 3a) and, in tandem with $C_{35}S/C_{34}S$, suggests a clay-rich source rock (Peters et al., 2005).

The C_{19}/C_{23} tricyclic terpane ratio is used to distinguish between algal/microbial and terrigenous sources of OM because C_{19} is mainly derived from higher plants, whereas C_{23} is a predominant component of algal and microbial OM (Simoneit, 1977). High values of the ratio indicate oils derived from source rocks containing significant amounts of terrigenous OM, whereas oils originating from algal/microbial OM have low values. All samples (Boulby oils and Malton 4 dolomites) have low values (0.03 – 0.24; Table 3a) of the C_{19}/C_{23} ratio suggesting that OM is dominated by marine algal/microbial components.

The diasterane/sterane ratio also helps to distinguish oil from carbonate versus clastic source rock (Mello et al., 1988). High diasterane/sterane ratios are typically interpreted to be derived from a clay-rich source rock but high ratios have also been observed in extracts from organic-lean and clay-poor carbonate rock (Palacas et al., 1984; Moldowan et al., 1991), or they might result from high thermal maturity or heavy biodegradation (Seifert and Moldowan, 1978, 1979), also in the case of coals (Killops et al., 1994). The diasterane/sterane ratio (C_{27} and C_{29}) in all oil samples of between 0.3 and 0.9 and in KAF dolomite samples (0.3 – 4) suggests a carbonate-evaporite source rock with an abundant clay (marl) content (Table 3b). Importantly, a very characteristic biomarker for all Boulby oil samples is an unusually abundant C_{29} 24-ethyl-13β(H),17α(H)-diacholestane (20S) (Fig. 9). High abundances of C_{29} diasteranes (20S + 20R) have also been found in the Middle Jurassic Sanjianfang Formation oil generated from the Xishanyao Formation coal interbedded with shale (Sun et al., 2000). Therefore, given the high diasterane/sterane ratio in Boulby oil samples (Table 3b), we tentatively assign C_{29} 24-ethyl-13β(H),17α(H)-diacholestane (20S) to the clay source.

In summary, Boulby oil was generated from a source rock deposited under suboxic-anoxic marine carbonate-evaporite-clayey conditions similar to the depositional conditions of KAF lagoonal facies. The absence of 28,30-bisnorhopane (BNH) commonly found in KCF kerogen and oil in the North Sea (Grantham et al., 1980) argues against an Upper Jurassic

564   source rock for Boulby oil, although this should be treated with caution because BNH

565   decreases with increasing thermal maturity (Peters et al., 2005). However, the BNH/$17\alpha\beta$-C_{30}

566   ratio (0.01-0.06) applied as a facies parameter is typical of Zechstein Main Dolomite oil in

567   other parts of the SPB (Petersen et al., 2016; Słowakiewicz, 2016; Słowakiewicz et al., 2018),

568   although BNH was not detected in KAF dolomite samples either. Gammacerane, commonly

569   invoked as evidence for a stratified water column in marine and non-marine depositional

570   environments and/or specifically for hypersalinity (Moldowan et al., 1985; Jiamo et al., 1986;

571   Sinninghe Damsté et al., 1995), is also absent. This suggests that OM may not have been

572   deposited under high-salinity conditions or gammacerane has not been preserved. The

573   predominance of $17\alpha\beta$-C_{34} or C_{35} homologues has been found to be characteristic of

574   Zechstein oil (Słowakiewicz et al., 2018), and dominance of $17\alpha\beta$-C_{32} and C_{35} homologues

575   occurs in Malton 4 KAF lagoonal carbonate rocks (Słowakiewicz et al., 2016, and this study).

576

m/z 217   GC-MS   A

oil sample 2

diaC$_{27}$βα S diaC$_{27}$βα R
diaC$_{27}$αβ S diaC$_{28}$βα S
diaC$_{28}$βα R
C$_{27}$αα S
C$_{27}$αα R
diaC$_{29}$βα S
diaC$_{29}$βα R
diaC$_{29}$αβ S
C$_{28}$ββ R
C$_{29}$αα S C$_{29}$ββ R

Malton 4, 4120 ft

diaC$_{27}$βα S
diaC$_{27}$βα R
diaC$_{27}$αβ S
diaC$_{28}$βα S diaC$_{27}$αβ R
diaC$_{28}$βα R
C$_{27}$αα S + methyl diaC$_{29}$αβ S
C$_{27}$ββ S diaC$_{29}$βα S + C$_{27}$ββ R
diaC$_{29}$βα R C$_{27}$αα R
C$_{28}$αα S
C$_{28}$ββ S C$_{28}$ββ R
C$_{28}$αα R
C$_{29}$αα S
C$_{29}$ββ S C$_{29}$ββ R
C$_{29}$αα R

Retention time ⟶

m/z 217   GC-MS   B

oil sample 1

diaC$_{27}$βα S
diaC$_{27}$βα R
diaC$_{27}$αβ S diaC$_{28}$βα S
diaC$_{28}$βα R
C$_{27}$αα S
C$_{27}$αα R
diaC$_{29}$βα S
diaC$_{29}$βα R
diaC$_{29}$αβ S
C$_{28}$ββ R
C$_{28}$αα R
C$_{29}$αα S C$_{29}$ββ R
C$_{29}$ββ S
C$_{29}$αα R

372→217   GC-MS/MS

diaC$_{27}$βα S
diaC$_{27}$βα R
diaC$_{27}$αβ R
diaC$_{27}$αβ S
C$_{27}$αα S C$_{27}$ββ R
C$_{27}$ββ S
C$_{27}$αα R

386→217

methyl diaC$_{28}$βα S
methyl diaC$_{28}$βα R
diaC$_{28}$αβ R
diaC$_{28}$αβ S
C$_{28}$αα S
C$_{28}$ββ S C$_{28}$ββ R
C$_{28}$αα R

400→217

diaC$_{29}$βα S
diaC$_{29}$βα R
diaC$_{29}$αβ R
diaC$_{29}$αβ S
C$_{29}$αα S
C$_{29}$ββ R C$_{29}$ββ S
C$_{29}$αα R

Retention time ⟶

578   **Fig. 9.** Sterane mass chromatograms (GC-MS and GC-MS/MS) for Boulby oil and Malton 4 KAF samples. (A)

579   Boulby oil sample 2 and Malton 4 lagoonal facies sample are given for comparison; (B) Note that Boulby oil

580   samples have elevated C_{29} 24-ethyl-13β(H),17α(H)-diacholestane (20S) tentatively assigned to high abundance

581   of clay-rich organic matter.

582

583   4.3.4. 3D seismic and fluid migration

584   Interpretation of the seismic data cube resulted in the definition of three main structural

585   trends (Figs. 10, 11).
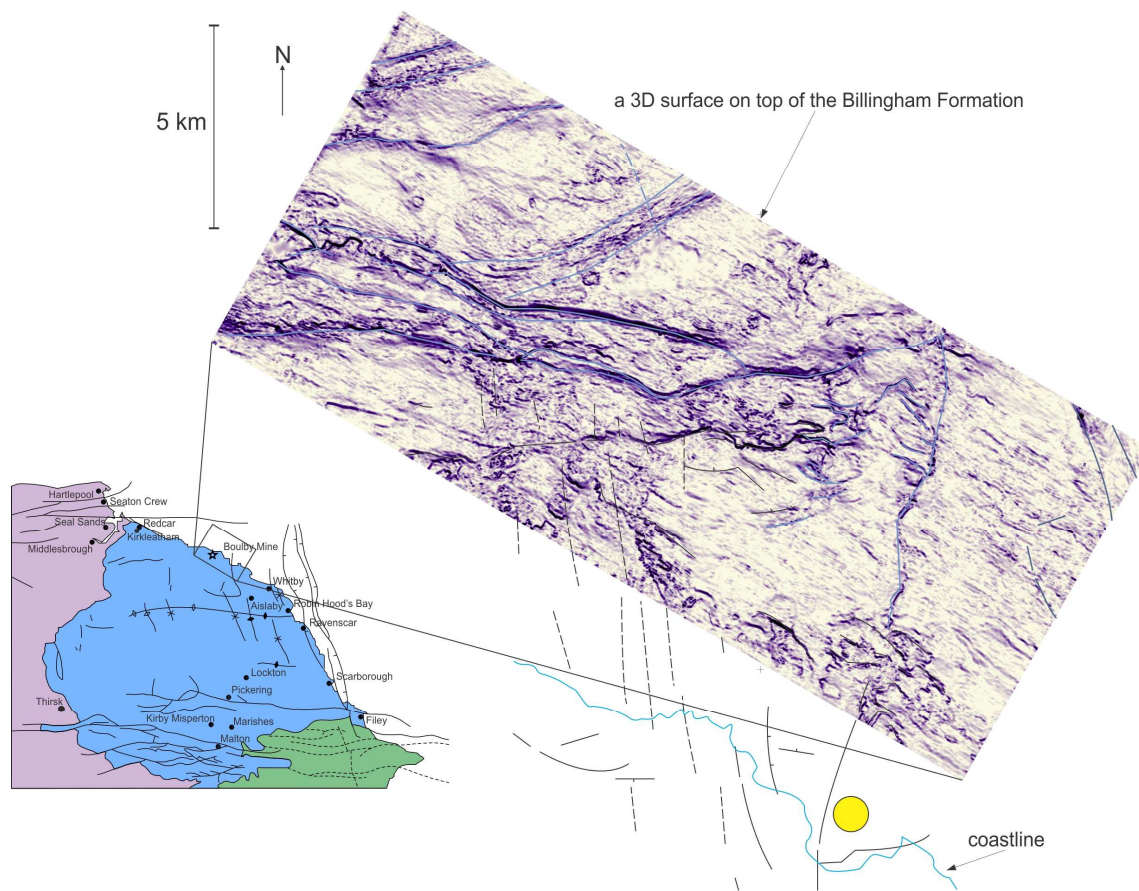
586

587   **Fig. 10.** Dip map highlighting the regional context and variation in dips. The darker areas of strong dip highlight

588   major structures affecting the top of the Billingham Formation anhydrite (EZ3A). Sampling location is marked
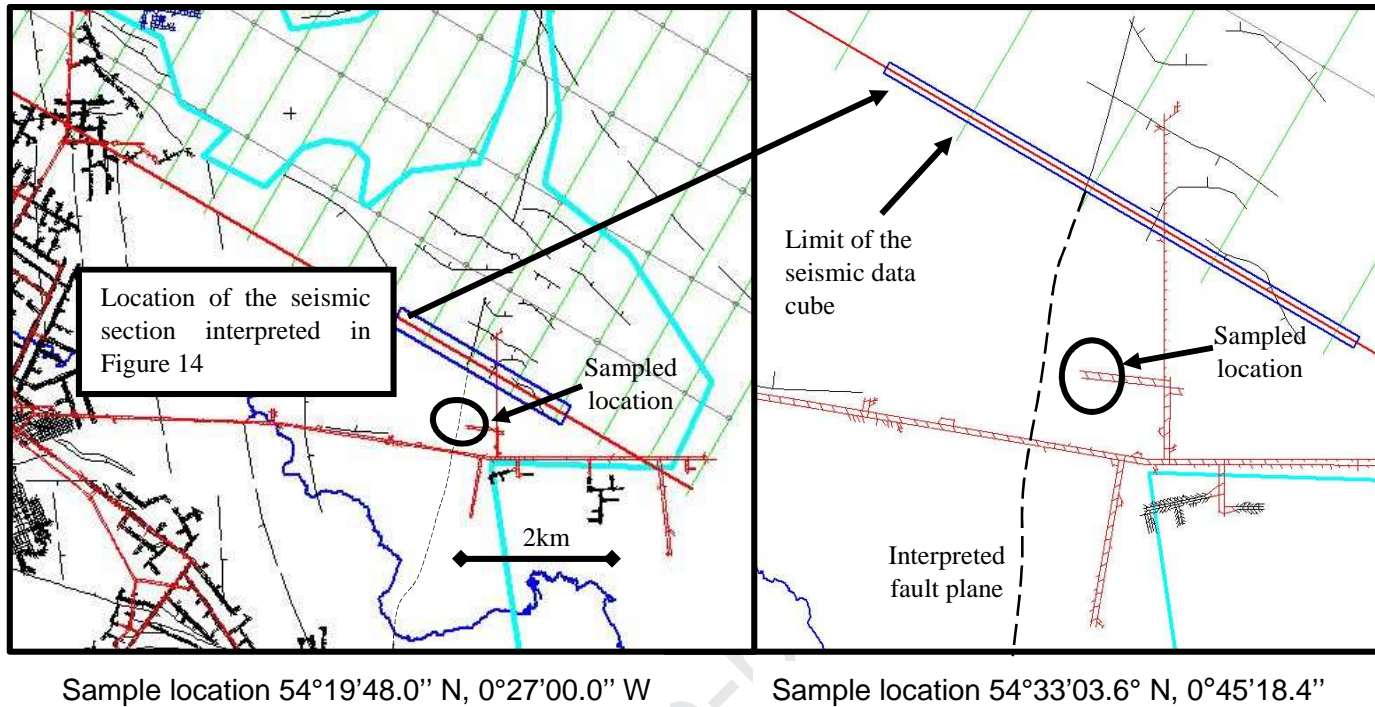
589   by the yellow circle.

590

591

592

593

594

595

Location of the seismic section interpreted in Figure 14

Sampled location

Limit of the seismic data cube

Sampled location

Interpreted fault plane

2km

Sample location 54°19'48.0'' N, 0°27'00.0'' W   Sample location 54°33'03.6° N, 0°45'18.4''

Fig. 11. Map of the Boulby oil sampling location and its relation to the seismic survey area (inset). Major structural features are highlighted (courtesy of ICL UK). Light blue line is the 'seismically quiet' area identified by the 3D survey.

1) East-west trending faults which cut across the offshore area in the centre of the data cube: There is an indication of separation along these faults between shallower and deeper sections where plastic flow of the halite, marl and potash intervals within the upper part of the EZ3 and lower EZ4 cycles accommodates brittle displacement in the underlying sequence (Fig. 10, Hardy, 2011 unpublished).

2) Northeast-southwest faults (Fig. 12): This system is composed of deep level *en-echelon* and shallow through-going components. There are complex interactions with the east-west faulting and seismic data indicate extensive thinning and possible absence of halite/potash at the junction of the two fault systems.

Composite pressure transfer fault model
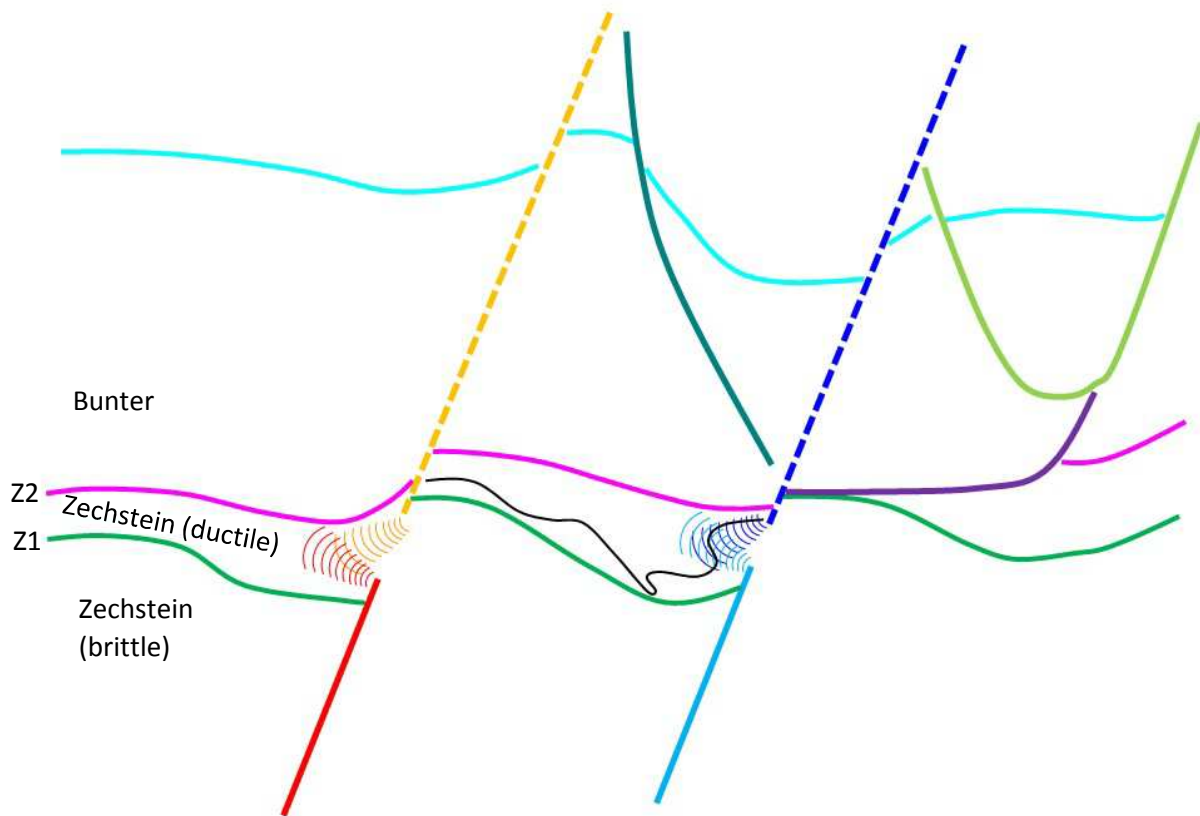
Fig. 12. Current cross-section model of the faults affecting the various strata within the study area, highlighting the observed dissipation of fault offset by plastic strata in the two Zechstein horizons (Z1 + Z2) as well as the brittle fracturing in anhydrite and dolomite below (Hardy, 2011 unpublished). Model has planar (or near planar) faulting above and below which effectively terminates on entering the plastic, mobile Zechstein rock. The energy of the fault movement dissipates as a pressure front through the rock causing flow in the mobile units (i.e., potash, marls) and fracturing in the interstitial brittle units (i.e., dolomite) (courtesy of Israel Chemicals Ltd).

3) North-south faults: These form part of the Peak Fault system (Milsom and Rawson, 1989) and are the most relevant trend for this study. These N-S faults are known to have been active during Jurassic times, i.e., they show evidence for synsedimentary movements. Other synsedimentary N-S faults in the Cleveland Basin include the Whitby Harbour Fault and the Runswick Bay Fault, relatively close to the Boulby Mine. The N-S fault structure interacts directly with the area from which the oil described herein and that previously encountered by mining were collected. Although direct intersection of the fault plane by drilling is limited, significant occurrences of thinned/absent strata, washouts, collapse breccias and evidence for geologically high fluid flux are common throughout the region surrounding this system over

many kilometres. These features indicate that the Peak Fault system has acted as a fluid pathway for brine and oil, presumably sourced from depth and localised within the Boulby Halite Formation.

Numerous H_2S and hydrocarbon-rich halite horizons and seeps from anhydrite were detected whilst crossing this area with exploratory wells. All workings mined across the fault were subject to ingress of light oil and gas not normally encountered elsewhere in the mine, the majority of which appear to be trapped at or below the Boulby Potash Member (EZ3K) level.

Further evidence of the upward migration of fluids within the EZ3 halite was demonstrated when mining revealed a series of pillar-like bodies of white coarse-grained halite within the normal laminar halite strata (EZ3Na); these structures demonstrate cross-cutting relationships to the EZ3 halite and fragments of the surrounding rock could be seen breaking off at the tip of the structure (Fig. 13).

Adjacent seismic sections (Fig. 14) illustrate this zone of faulting and disturbance. Breaks in a number of stratigraphic markers, in particular the Billingham Formation anhydrite, can be picked out and a zone of ductile deformation which can be seen extending ~100-200 m away from the fault.
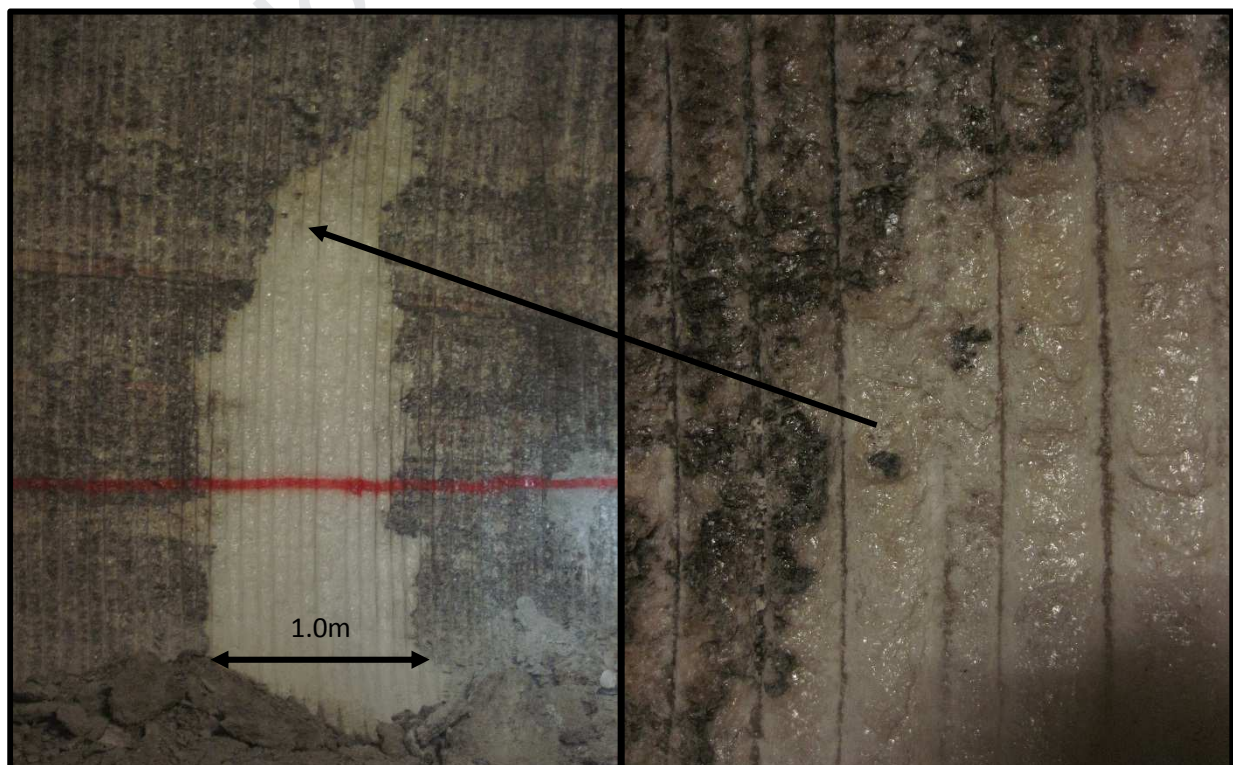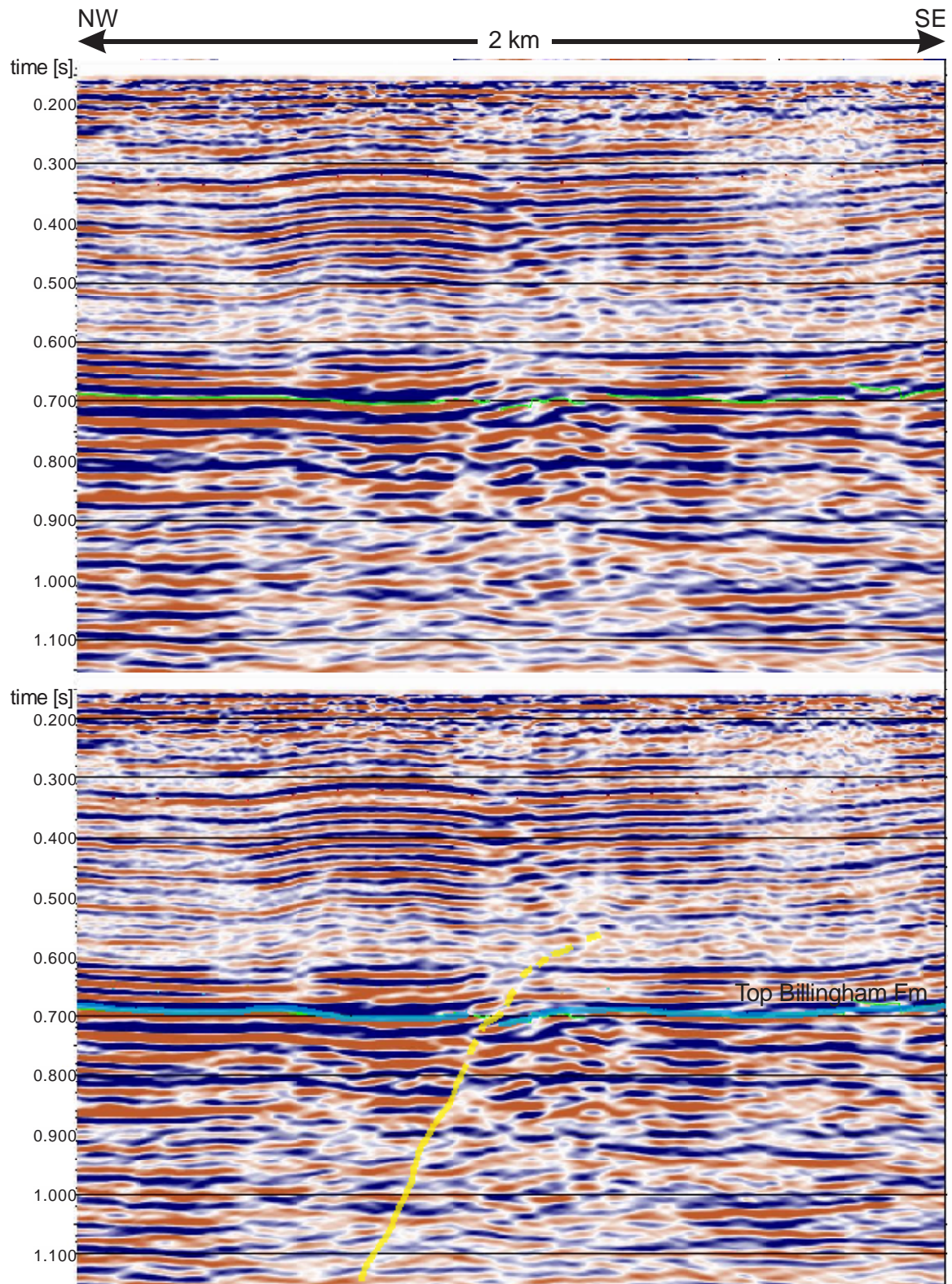

1.0m

671

672

673 **Fig. 13.** Two photographs illustrating a cross-cutting white halite pillar with associated hydrocarbon residue

674 trapped towards the tip within the EZ3Na halite, Boulby Mine. Approximate field of view: 3.5m H x 2.0m W

675 (photograph courtesy of Israel Chemicals Ltd).

676

Fig. 14. Clean and interpreted seismic section pair through the fault zone adjacent to the sampling location. Top of the Billingham Formation anhydrite marked approximately half-way down the section with the fault picked out in yellow. Vertical scale: time in seconds (sections courtesy of Israel Chemicals Ltd).

682

5. Discussion

683

684   From time to time oil is encountered during mining operations at Boulby Potash Mine on

685   the coast of Yorkshire. 'Live' flowing oil was encountered in early September 2018 and

686   sampled immediately. The analytical results of biomarker distributions demonstrate clearly

687   that Boulby oil was generated locally from three likely source rocks: the Brotherton

688   Formation (EZ3Ca = Plattendolomit), the KAF (EZ2Ca = Hauptdolomit) and Namurian oil

689   shale, although, as noted earlier, one other possibility is OM from microbialites within

690   anhydrite facies, i.e., Hayton (EZ1A), Fordon (EZ2A) and Billingham (EZ3A) anhydrites.

691   The Brotherton Formation (26 m thick) consists of very dark grey to black fine-grained

692   muddy carbonate, mostly dolomite, and locally this rock contains dolopackstone formed by

693   the green alga *Calcinema*. The Brotherton is located some 50 m below the mine working

694   where the oil was collected, and it has been encountered in drilling for polyhalite (Z2 age)

695   which occurs just below that carbonate. The KAF carbonate is present 200 m below the halite

696   from which the oil drips, and here it is likely to be in a mid-outer ramp facies with a thickness

697   in the region of approximately 200 m, although the actual thickness has not been established.

698   This KAF facies has been examined from two boreholes in North Yorkshire, 30 km

699   (Lockton) and 50 km (Malton) south of the Boulby Mine (Fig. 1; Słowakiewicz et al., 2016,

700   and this study). Here, OM from Lockton KAF lower slope facies has high thermal maturity

701   (reduced or absent hopanes and steranes), likely resulting from burial diagenetic or

702   hydrothermal influence, but OM from Malton KAF lagoonal facies is within the peak oil

703   window for hydrocarbon generation. Distribution of n-alkanes in the latter is unimodal or

704   bimodal and n-C_{18} and n-C_{23} or n-C_{24} are the most abundant unless samples are biodegraded

705   or thermally altered. Gammacerane and BNH are absent; C_{32} and C_{35} homohopanes dominate

706   over C_{31} and C_{33} or C_{34} homologues, respectively, and C_{27} and/or C_{29} regular steranes are

707   predominant (Figs. 8,9). OM is clay-rich as also identified in Boulby oil samples. Hence,

708   most likely the lagoonal dolomite identified in the KAF might be the source rock for Boulby

709   oil. Such marly algal-microbial dolomite source rocks are well documented in Central

710   Europe and they form an important source rock for oil in the German and Polish sections of

711   the SPB (Słowakiewicz et al., 2018). However, never before has mature Zechstein oil been

712   found so far west.

713   Zechstein evaporites, which seal KAF's stratigraphic equivalents elsewhere in the SPB,

714   containing clay-rich chicken-wire anhydrite, have been interpreted as important contributors

715   to a source rock for Zechstein oil (Słowakiewicz et al., 2018). Yet, biomarker distributions

716   and their characteristics obtained from the Hartlepool Anhydrite (= Z1A, Werraanhydrit, 590-

717   1020 ft [179.8-310.9 m]) from Durham Offshore Borehole No. 1 do not match those of

718   Boulby oil; more data are needed to prove these rocks as a potential source rock for

719   petroleum in the North Sea (our unpublished data).

720   The second significant source rock for Boulby oil could be Namurian (Edale Shale

721   Group) oil shale. It was deposited in a distal pro-delta setting (Fraser et al., 1990) and hence

722   the OM is of predominantly terrigenous type. However, the high abundance of diasteranes

723   (particularly C_{29} diacholestane 20S) in the Boulby oil is more likely to be a reflection of a

724   marine clay rather than a terrigenous OM source; it is noteworthy that the OM in the KAF

725   dolomite samples is also of marine clay-rich type. Importantly, Namurian source rock in the

726   Boulby area is in both the peak oil and gas window (Fraser et al., 1990; Heath-Clarke et al.,

727   2016; Haarhoff et al., 2018); this is closely similar to the interpreted peak to late oil window

728   for hydrocarbon generation of the Boulby oil. However, the oil residues filling fractures in

729   the Devonian Weardale Granite in Co. Durham (100 km NW of Boulby), which were

730   probably derived from a mid-Carboniferous source rock (Baba et al., 2019) have significantly

731   different distributions of *n*-alkanes, steranes and hopanes compared to the Boulby oil and

732   KAF dolomite samples. In addition, Edale Shale Group oil shale has not been identified in

733   the close vicinity of the Boulby Mine and 41/18-1 mudrock samples. Finally, the structural

734   pattern in the Boulby area and presence of several fault systems would have created excellent

735   conduits for fluid migration from the Zechstein KAF source rock to more porous portions of

736   Brotherton Formation dolomite. As reported by Holmes (1991) and presented herein, the

737   presence of a reverse fault well exposed by mine workings (Fig. 13) results in a 35-m vertical

738   displacement of the Brotherton Formation dolomite and Z3 evaporites (anhydrite, halite and

739   potash beds) are draped over it. Boulby oil seeped from the Brotherton Formation carbonate

740   rocks when they were first encountered during drilling at the mine (Davison, 2009) so that the

741   oil must be migrating up from lower stratigraphic levels (KAF) into the Boulby Halite

742   through some transient faults, although Z3 anhydrite and halite would mostly act as seals.

743   The latter and, along with the underlying Roxby Formation marl, which is ~125 m thick in

744   the Boulby Mine area, may have prevented the Boulby oil from reaching the porous

745   Sherwood Sandstone Group strata above.

746 To date, the perceived primary exploration risk in the offshore area has been an absence
747 of an oil source rock. The presence of thermally mature Zechstein source rock in this western
748 UK sector of the North Sea is important because much of the recently offered exploration
749 acreage in the UK 30th and 31st Licencing rounds is just ~50 km east of the proven oil at
750 Boulby.

751

6. Conclusions

753 The investigated origin of the Boulby oil, seeping from fractures in the Boulby Halite
754 Formation rock salt, and based on its stable carbon isotopes, biomarker distributions and
755 structural pattern, is that it was likely derived from Zechstein 2 Kirkham Abbey Formation
756 sapropelic dolomite and reservoired by Zechstein 3 Brotherton Formation dolomite. The
757 thermal maturity of the analysed oil is in the peak to late oil window.

758 $\delta^{13}C$ values and biomarker signatures of saturated and aromatic hydrocarbon fractions
759 show that oil samples were not derived from Devonian or Late Jurassic source rocks. With
760 respect to source, a carbonate-evaporite depositional setting is indicated by the high
761 abundance of C_{32} and C_{34} homohopane homologues and EOP of C_{20-25} n-alkanes whereas
762 clay-rich (but not terrigenous) OM is implied by the abundant C_{29} ethyl-diacholestane 20S,
763 which seem to be characteristic biomarkers of the Boulby oil. The source rock was deposited
764 under marine and suboxic-anoxic conditions. Similar biomarker distributions (apart from
765 abundant C_{29} ethyl-diacholestane 20S) have been detected in Malton 4 KAF dolomite
766 samples, suggested to be the likely source rock for the Boulby oil.

767 Collectively, biomarker fingerprints and seismic data have allowed the identification of
768 depositional environment, OM source, thermal maturity and migration pathways of Boulby
769 oil in the Cleveland Basin.

770

Acknowledgements

776 share data regarding this work. We also acknowledge Ronaldo di Primio, Phil Welsh, Huan

777 Yang, Sean Paling and Lars Reuning for their additional support. Two anonymous reviewers

778 are thanked for their constructive reviews and suggestions to improve our manuscript. This

779 study was also partially supported by the Russian Government Programme of Competitive

780 Growth of the Kazan Federal University.

781

Author contributions

783 M.S. designed the project, analysed the data and wrote the manuscript. This study is partly

784 based on S.S.'s BSc thesis (Słama, 2019) supervised by M.S., which provided some

785 biomarker analyses. J.G. provided oil samples. A.K. performed the GC-FID and GC-MS. T.E.

786 and P.S. provided seismic and geological data and oil samples. J.G., S.S., M.M., M.E.T., I.P.

787 contributed to writing the article. All authors approved the manuscript.

788

References

790 Akinlua, A., Ajayi, T.R., Adeleke, B.B., 2006. Niger Delta oil geochemistry: Insight from light
791 hydrocarbons. Journal of Petroleum Science and Engineering 50, 308–314.
792 https://doi.org/10.1016/j.petrol.2005.12.003

793 Andrews, I.J., 2013. The Carboniferous Bowland Shale gas study: geology and resource estimation.
794 British Geological Survey for Department of Energy and Climate Change, London, UK.

795 Andrusevich, V.E., Engel, M.H., Zumberge, J.E., 2000. Effects of paleolatitude on the stable carbon
796 isotope composition of crude oils. Geology 28, 847–850. https://doi.org/10.1130/0091-
797 7613(2000)28<847:EOPOTS>2.0.CO;2

798 Andrusevich, V.E., Engel, M.H., Zumberge, J.E., Brothers, L.A., 1998. Secular, episodic changes in
799 stable carbon isotope composition of crude oils. Chemical Geology 152, 59–72.
800 https://doi.org/10.1016/S0009-2541(98)00096-5

801 Armstroff, A., 2004. Geochemical significance of biomarkers in Paleozoic coals, PhD dissertation.
802 Berlin.

803 Baba, M., Parnell, J., Bowden, S., Armstrong, J., Perez, M., Wang, X., 2019. Emplacement of oil in the
804 Devonian Weardale Granite of northern England. Proceedings of the Yorkshire Geological
805 Society 62, 229–237. https://doi.org/10.1144/pygs2018-008

806 Bailey, N.J.L., Burwood, R., Harriman, G.E., 1990. Application of pyrolysate carbon isotope and
807 biomarker technology to organofacies definition and oil correlation problems in North Sea
808 basins. Organic Geochemistry 16, 1157–1172. https://doi.org/10.1016/0146-6380(90)90151-
809 O

810 Barnard, P.C., Cooper, B.S., 1983. A review of geochemical data related to the Northwest European
811 Gas Province. Geological Society, London, Special Publications 12, 19–33.
812 https://doi.org/10.1144/GSL.SP.1983.012.01.04

813 Beach, F., Peakman, T.M., Abbott, G.D., Sleeman, R., Maxwell, J.R., 1989. Laboratory thermal
814 alteration of triaromatic steroid hydrocarbons. Organic Geochemistry 14, 109–111.
815 https://doi.org/10.1016/0146-6380(89)90024-7

816 Besly, B.M., 1998. Carboniferous, in: Glennie, K.W. (Ed.), Petroleum Geology of the North Sea.
817   Blackwell Science Ltd, pp. 104–136.
818 Brassell, S.C., Eglinton, G., Sheng, G., Fu, J., 1988. Biological markers in lacustrine Chinese oil shales.
819   Geological Society, London, Special Publications 40, 299–308.
820   https://doi.org/10.1144/GSL.SP.1988.040.01.24
821 Burgess, P.M., Gayer, R.A., 2000. Late Carboniferous tectonic subsidence in South Wales:
822   implications for Variscan basin evolution and tectonic history in SW Britain. Journal of the
823   Geological Society 157, 93–104. https://doi.org/10.1144/jgs.157.1.93
824 Chadwick, R.A., Holliday, D.W., Holloway, S., Hulbert, A.G., 1993. The evolution and hydrocarbon
825   potential of the Northumberland–Solway Basin. Geological Society, London, Petroleum
826   Geology Conference series 4, 717–726. https://doi.org/10.1144/0040717
827 Chung, H.M., Rooney, M.A., Toon, M.B., Claypool, G.E., 1992. Carbon isotope composition of marine
828   crude oils. AAPG Bulletin 76, 1000–1007.
829 Clark, J.P., Philp, R.P., 1989. Geochemical characterization of evaporite and carbonate depositional
830   environments and correlation of associated crude oils in the Black Creek Basin, Alberta.
831   Bulletin of Canadian Petroleum Geology 37, 401–416.
832 Connan, J., Cassou, A.M., 1980. Properties of gases and petroleum liquids derived from terrestrial
833   kerogen at various maturation levels. Geochimica et Cosmochimica Acta 44, 1–23.
834   https://doi.org/10.1016/0016-7037(80)90173-8
835 Cooper, B.S., Barnard, P.C., Telnaes, N., 1995. The Kimmeridge Clay Formation of the North Sea, in:
836   Katz, B.J. (Ed.), Petroleum Source Rocks. Springer Berlin Heidelberg, Berlin, Heidelberg, pp.
837   89–110. https://doi.org/10.1007/978-3-642-78911-3_6
838 Corfield, S.M., Gawthorpe, R.L., Gage, M., Fraser, A.J., Besly, B.M., 1996. Inversion tectonics of the
839   Variscan foreland of the British Isles. Journal of the Geological Society 153, 17–32.
840   https://doi.org/10.1144/gsjgs.153.1.0017
841 Craig, J., Gluyas, J., Laing, C., Schofield, P., 2015. Hardstoft – Britain's first oil field. Search and
842   Discovery Article #70188.
843 Creaney, S., Jones, J.M., Holliday, D.W., Robson, P., 1980. The occurrence of bitumen in the Great
844   Limestone around Matfen, Northumberland – its characterisation and possible genesis.
845   Proceedings of the Yorkshire Geological Society 43, 69–79.
846   https://doi.org/10.1144/pygs.43.1.69
847 Daniels, S.E., Tucker, M.E., Mawson, M.J., Holdsworth, R.E., Long, J.J., Gluyas, J.G., Jones, R.R., 2020.
848   Nature and origin of collapse breccias in the Zechstein of NE England: local observations with
849   cross-border petroleum exploration and production significance, across the North Sea.
850   Geological Society, London, Special Publications 494. https://doi.org/10.1144/SP494-2019-
851   140
852 Davison, I., 2009. Faulting and fluid flow through salt. Journal of the Geological Society 166, 205–216.
853   https://doi.org/10.1144/0016-76492008-064
854 de Leeuw, J.W., Sinninghe Damsté, J.S., 1990. Organic sulphur compounds and other biomarkers as
855   indicators of palaeosalinity, in: Orr, W.L., White, C.M. (Eds.), Geochemistry of Sulfur in Fossil
856   Fuels, ACS Symposium Series. American Chemical Society, pp. 417–443.
857   https://doi.org/10.1021/bk-1990-0429.ch024
858 DECC, 2013. The hydrocarbon prospectivity of Britain's onshore basins. Department of Energy &
859   Climate Change, 86p.
860 Dembicki, H., Meinschein, W.G., Hattin, D.E., 1976. Possible ecological and environmental
861   significance of the predominance of even-carbon number C20-C30n-alkanes. Geochimica et
862   Cosmochimica Acta 40, 203–208. https://doi.org/10.1016/0016-7037(76)90177-0
863 Duguid, C., Underhill, J.R., 2010. Geological controls on Upper Permian Plattendolomit Formation
864   reservoir prospectivity, Wissey Field, UK Southern North Sea. Petroleum Geoscience 16,
865   331–348. https://doi.org/10.1144/1354-0793/10-021

866 Evans, D., Graham, C., Armour, A., Bathurst, P. (Eds.), 2003. The millennium atlas: Petroleum geology
867   of the Central & Northern North Sea. Geological Society of London.
868 Fisher, D.J., Holloway, P.J., Richmond, D.V., 1972. Fatty acid and hydrocarbon constituents of the
869   surface and wall lipids of some fungal spores. Microbiology, 72, 71–78.
870   https://doi.org/10.1099/00221287-72-1-71
871 Fraser, A.J., Gawthorpe, R.L., 1990. Tectono-stratigraphic development and hydrocarbon habitat of
872   the Carboniferous in northern England. Geological Society, London, Special Publications 55,
873   49–86. https://doi.org/10.1144/GSL.SP.1990.055.01.03
874 Fraser, A.J., Nash, D.F., Steele, R.P., Ebdon, C.C., Fraser, A.J., 1990. A regional assessment of the
875   intra-Carboniferous play of Northern England. Geological Society, London, Special
876   Publications 50, 417–440. https://doi.org/10.1144/GSL.SP.1990.050.01.26
877 French, K.L., Sepúlveda, J., Trabucho-Alexandre, J., Gröcke, D.R., Summons, R.E., 2014. Organic
878   geochemistry of the early Toarcian oceanic anoxic event in Hawsker Bottoms, Yorkshire,
879   England. Earth and Planetary Science Letters 390, 116–127.
880   https://doi.org/10.1016/j.epsl.2013.12.033
881 Fuex, A.N., 1977. The use of stable carbon isotopes in hydrocarbon exploration. Journal of
882   Geochemical Exploration 7, 155–188. https://doi.org/10.1016/0375-6742(77)90080-2
883 Gautier, D.L., 2005. Kimmeridgian shales total petroleum system of the North Sea Graben Province.
884   U.S. Geological Survey Bulletin 2204-C, 24p.
885 Glennie, K.W., Higham, J., Stemmerik, L., 2003. Permian, in: Evans, D., Graham, C., Armour, A.,
886   Bathurst, P. (Eds.), The Millenium Atlas: Petroleum Geology of the Central and Northern
887   North Sea. Geological Society of London, London, pp. 91–103.
888 Glennie, K.W., Underhill, J.R., 1998. Origin, development and evolution of structural styles, in:
889   Glennie, K.W. (Ed.), Petroleum Geology of the North Sea. Blackwell Science Ltd, Oxford, pp.
890   42–84.
891 Gluyas, J., Bowman, M., 1997. Edale no. 1 oilwell, Derbyshire, UK, 1938. Marine and Petroleum
892   Geology 14, 191–199. https://doi.org/10.1016/S0264-8172(96)00066-9
893 Grantham, P.J., Posthuma, J., de Groot, K., 1980. Variation and significance of the C27 and C28
894   triterpane content of a North Sea core and various North Sea crude oils. Physics and
895   Chemistry of the Earth 12, 29–38. https://doi.org/10.1016/0079-1946(79)90086-7
896 Gross, D., Sachsenhofer, R.F., Bechtel, A., Pytlak, L., Rupprecht, B., Wegerer, E., 2015. Organic
897   geochemistry of Mississippian shales (Bowland Shale Formation) in central Britain:
898   Implications for depositional environment, source rock and gas shale potential. Marine and
899   Petroleum Geology 59, 1–21. https://doi.org/10.1016/j.marpetgeo.2014.07.022
900 Haarhoff, M.Q., Hughes, F., Heath-Clarke, M., Harrison, D., Taylor, C., Ware, D.L., Emms, G.G.,
901   Mortimer, A., 2018. The history of hydrocarbon exploration and development in North
902   Yorkshire. Geological Society, London, Special Publications 465, 119–136.
903   https://doi.org/10.1144/SP465.12
904 Han, J., Calvin, M., 1969. Hydrocarbon Distribution of Algae and Bacteria, and Microbiological
905   Activity in Sediments. PNAS 64, 436–443. https://doi.org/10.1073/pnas.64.2.436
906 Hardy, N., 2011. Summary and conclusion report for 3D interpretation HEC. Internal ICL report,
907   unpublished.
908 Heath-Clarke, M., Taylor, K., Harrison, D., Fogg, A., Hughes, F., Haarhoff, M., Mortimer, A., 2016. The
909   characterization of unconventional reservoirs in the Bowland sequence using onshore 3D
910   seismic data, Cleveland Basin, UK. First Break 34, 45–52.
911 Holba, A.G., Dzou, L.I.P., Hickey, J.J., Franks, S.G., May, S.J., Lenney, T., 1996. Reservoir geochemistry
912   of South Pass 61 Field, Gulf of Mexico: compositional heterogeneities reflecting filling history
913   and biodegradation. Organic Geochemistry, Reservoir and Production Geochemistry 24,
914   1179–1198. https://doi.org/10.1016/S0146-6380(96)00101-5

915 Holliday, D.W., 1999. Palaeotemperatures, thermal modelling and depth of burial studies in northern
916   and eastern England. Proceedings of the Yorkshire Geological and Polytechnic Society 52,
917   337–352. https://doi.org/10.1144/pygs.52.4.337

918 Holmes, R., 1991. Some aspects of the geology of the potash seam at Boulby Mine. Journal of the
919   Open University Geological Society 12, 77–88.

920 Huc, A.Y., Irwin, H., Schoell, M., 1985. Organic matter quality changes in an Upper Jurassic shale
921   sequence from the Viking Graben, in: Thomas, B.M. (Ed.), Petroleum Geochemistry in
922   Exploration of the Norwegian Shelf. Springer Netherlands, pp. 179–183.

923 Hughes, F., Harrison, D., Haarhoff, M., Howlett, P., Pearson, A., Ware, D., Taylor, C., Emms, G.,
924   Mortimer, A., 2018. The unconventional Carboniferous reservoirs of the Greater Kirby
925   Misperton gas field and their potential: North Yorkshire's sleeping giant. Geological Society,
926   London, Petroleum Geology Conference series 8, 611. https://doi.org/10.1144/PGC8.5

927 Husmo, T., Hamar, G.P., Høiland, O., Johannessen, E.P., Rømuld, A., Spencer, A., Titterton, R., 2002.
928   Lower and Middle Jurassic, in: Evans, D., Graham, C., Armour, A., Bathurst, P. (Eds.), The
929   Millenium Atlas: Petroleum Geology of the Central and Northern North Sea. Geological
930   Society of London, London, pp. 129–155.

931 Imber, J., Armstrong, H., Clancy, S., Daniels, S., Herringshaw, L., McCaffrey, K., Rodrigues, J.,
932   Trabucho-Alexandre, J., Warren, C., 2014. Natural fractures in a United Kingdom shale
933   reservoir analog, Cleveland Basin, northeast England natural fractures, Cleveland Basin.
934   AAPG Bulletin 98, 2411–2437. https://doi.org/10.1306/07141413144

935 Jiamo, F., Guoying, S., Pingan, P., Brassell, S.C., Eglinton, G., Jigang, J., 1986. Peculiarities of salt lake
936   sediments as potential source rocks in China. Organic Geochemistry 10, 119–126.
937   https://doi.org/10.1016/0146-6380(86)90015-X

938 Jiang, Z., Philp, R.P., Lewis, C.A., 1988. Fractionation of biological markers in crude oils during
939   migration and the effects on correlation and maturation parameters. Organic Geochemistry
940   13, 561–571. https://doi.org/10.1016/0146-6380(88)90076-9

941 Johnson, G.A.L., Somerville, I.D., Tucker, M.E., Cózar, P., 2011. Carboniferous stratigraphy and
942   context of the Seal Sands No. 1 Borehole, Teesmouth, NE England: the deepest onshore
943   borehole in Great Britain. Proceedings of the Yorkshire Geological Society 58, 173.
944   https://doi.org/10.1144/pygs.58.3.231

945 Jones, J.G., 1969. Studies on lipids of soil micro-organisms with particular reference to hydrocarbons.
946   Microbiology, 59, 145–152. https://doi.org/10.1099/00221287-59-2-145

947 Kara-Gülbay, R., Korkmaz, S., 2008. Organic geochemistry, depositional environment and
948   hydrocarbon potential of the Tertiary oil shale deposits in NW Anatolia, Turkey. Oil Shale 25,
949   444–464.

950 Kemp, S.J., Merriman, R.J., Bouch, J.E., 2005. Clay mineral reaction progress – the maturity and burial
951   history of the Lias Group of England and Wales. Clay Minerals 40, 43–61.
952   https://doi.org/10.1180/0009855054010154

953 Kent, P.E., 1980. Subsidence and uplift in east Yorkshire and Lincolnshire: a double inversion.
954   Proceedings of the Yorkshire Geological Society 42, 505–524.
955   https://doi.org/10.1144/pygs.42.4.505

956 Killops, S.D., Woolhouse, A.D., Weston, R.J., Cook, R.A., 1994. A geochemical appraisal of oil
957   generation in the Taranaki Basin, New Zealand. AAPG Bulletin 78, 1560–1585.

958 Kombrink, H., Besly, B., Collinson, J., den Hartog Jager, D., Drozdzewski, G., Dusar, M., Hoth, P.,
959   Pagnier, H., Stemmerik, L., Waksmnundzka, M., Wrede, V., 2010. Carboniferous, in:
960   Doornenbal, H., Stevenson, A. (Eds.), Petroleum Geological Atlas of the Southern Permian
961   Basin Area. EAGE Publications b.v. (Houten), pp. 81–99.

962 Mackenzie, A.S., Hoffmann, C.F., Maxwell, J.R., 1981. Molecular parameters of maturation in the
963   Toarcian shales, Paris Basin, France—III. Changes in aromatic steroid hydrocarbons.
964   Geochimica et Cosmochimica Acta 45, 1345–1355. https://doi.org/10.1016/0016-
965   7037(81)90227-1

966 Mackenzie, A.S., Mackenzie, A.S., 1984. Applications of biological markers in petroleum
967   geochemistry, in: Brooks, J., Welte, D. (Eds.), Advances in Petroleum Geochemistry.
968   Academic Press, London, pp. 115–214. https://doi.org/10.1016/B978-0-12-032001-1.50008-
969   0
970 Mackenzie, A.S., Maxwell, J.R., Coleman, M.L., Deegan, C.E., 1983. Biological marker and isotope
971   studies of North Sea crude oils and sediments, in: WPC-20104. Presented at the 11th World
972   Petroleum Congress, Proceedings of the 11th World Petroleum Congress, Geology
973   Exploration Reserves, WPC, pp. 45–56.
974 Mackenzie, A.S., Patience, R.L., Maxwell, J.R., Vandenbroucke, M., Durand, B., 1980. Molecular
975   parameters of maturation in the Toarcian shales, Paris Basin, France—I. Changes in the
976   configurations of acyclic isoprenoid alkanes, steranes and triterpanes. Geochimica et
977   Cosmochimica Acta 44, 1709–1721. https://doi.org/10.1016/0016-7037(80)90222-7
978 Mello, M.R., Telnaes, N., Gaglianone, P.C., Chicarelli, M.I., Brassell, S.C., Maxwell, J.R., 1988. Organic
979   geochemical characterisation of depositional palaeoenvironments of source rocks and oils in
980   Brazilian marginal basins. Organic Geochemistry 13, 31–45. https://doi.org/10.1016/0146-
981   6380(88)90023-X
982 Milsom, J., Rawson, P.F., 1989. The Peak Trough – a major control on the geology of the North
983   Yorkshire coast. Geological Magazine 126, 699–705.
984   https://doi.org/10.1017/S0016756800007007
985 Moldowan, J.M., Lee, C.Y., Watt, D.S., Jeganathan, A., Slougui, N.-E., Gallegos, E.J., 1991. Analysis and
986   occurrence of C26-steranes in petroleum and source rocks. Geochimica et Cosmochimica
987   Acta 55, 1065–1081. https://doi.org/10.1016/0016-7037(91)90164-Z
988 Moldowan, J.M., Seifert, W.K., Gallegos, E.J., 1985. Relationship between petroleum composition
989   and depositional environment of petroleum source rocks. AAPG Bulletin 69, 1255–1268.
990 Palacas, J.G., Anders, D.E., King, J.D., 1984. South Florida Basin—A prime example of carbonate
991   source rocks of petroleum, in: Palacas, J.G. (Ed.), Petroleum Geochemistry and Source Rock
992   Potential of Carbonate Rocks. AAPG Studies in Geology 18, pp. 71–96.
993   https://doi.org/10.1306/St18443C6
994 Parnell, J., 1988. Lacustrine petroleum source rocks in the Dinantian Oil Shale Group, Scotland: a
995   review. Geological Society, London, Special Publications 40, 235–246.
996   https://doi.org/10.1144/GSL.SP.1988.040.01.20
997 Peters, K.E., Moldowan, J.M., 1991. Effects of source, thermal maturity, and biodegradation on the
998   distribution and isomerization of homohopanes in petroleum. Organic Geochemistry 17, 47–
999   61. https://doi.org/10.1016/0146-6380(91)90039-M
1000 Peters, K.E., Moldowan, J.M., Driscole, A.R., Demaison, G.J., 1989. Origin of Beatrice oil by co-
1001   sourcing from Devonian and Middle Jurassic source rocks, Inner Moray Firth, United
1002   Kingdom. AAPG Bulletin 73, 454–471.
1003 Peters, K.E., Walters, C.C., Moldowan, J.M., 2005. The Biomarker Guide. Biomarkers and Isotopes in
1004   Petroleum Exploration and Earth History vol. 2. Cambridge University Press, Cambridge,
1005   1155p. https://doi.org/10.1017/CBO9781107326040
1006 Petersen, H.I., Hertle, M., Juhasz, A., Krabbe, H., 2016. Oil family typing, biodegradation and source
1007   rock affinity of liquid petroleum in the Danish North Sea. Journal of Petroleum Geology 39,
1008   247–268. https://doi.org/10.1111/jpg.12645
1009 Pletsch, T., Appel, J., Botor, D., Clayton, C., Duin, E., Faber, E., Górecki, W., Kombrink, H., Kosakowski,
1010   P., Kuper, G., Kus, J., Lutz, R., Mathiesen, A., Ostertag-Henning, C., Papiernik, B., Bergen, F.,
1011   2010. Petroleum generation and migration, in: Doornenbal, H., Stevenson, A. (Eds.),
1012   Petroleum Geological Atlas of the Southern Permian Basin Area. EAGE Publications b.v.
1013   (Houten), pp. 225–253.
1014 Powell, J.H., 2010. Jurassic sedimentation in the Cleveland Basin: a review. Proceedings of the
1015   Yorkshire Geological Society 58, 21–72. https://doi.org/10.1144/pygs.58.1.278
1016 Rawson, P.F., Wright, J.K., 2018. The Yorkshire coast, 4th ed. Geologists' Association Guides 34, 178p.

1017 Rawson, P.F., Wright, J.K., 1995. Jurassic of the Cleveland Basin, North Yorkshire, in: Taylor, P.D. (Ed.),
1018   Field Geology of the British Jurassic. Geological Society, London, pp. 173–208.

1019 Requejo, A.G., Allan, J., Creaney, S., Gray, N.R., Cole, K.S., 1992. Aryl isoprenoids and diaromatic
1020   carotenoids in Paleozoic source rocks and oils from the Western Canada and Williston Basins.
1021   Organic Geochemistry 19, 245–264. https://doi.org/10.1016/0146-6380(92)90041-U

1022 Scotchman, I.C., 1991. Kerogen facies and maturity of the Kimmeridge Clay Formation in southern
1023   and eastern England. Marine and Petroleum Geology 8, 278–295.
1024   https://doi.org/10.1016/0264-8172(91)90082-C

1025 Seifert, W.K., Moldowan, J.M., 1980. The effect of thermal stress on source-rock quality as measured
1026   by hopane stereochemistry. Physics and Chemistry of the Earth 12, 229–237.
1027   https://doi.org/10.1016/0079-1946(79)90107-1

1028 Seifert, W.K., Moldowan, J.M., 1979. The effect of biodegradation on steranes and terpanes in crude
1029   oils. Geochimica et Cosmochimica Acta 43, 111–126. https://doi.org/10.1016/0016-
1030   7037(79)90051-6

1031 Seifert, W.K., Moldowan, J.M., 1978. Applications of steranes, terpanes and monoaromatics to the
1032   maturation, migration and source of crude oils. Geochimica et Cosmochimica Acta 42, 77–95.
1033   https://doi.org/10.1016/0016-7037(78)90219-3

1034 Shanmugam, G., 1985. Significance of coniferous rain forests and related organic matter in
1035   generating commercial quantities of oil, Gippsland Basin, Australia. AAPG Bulletin 69, 1241–
1036   1254.

1037 Shen, G., Fan, S., Lin, D., Su, N., Zhou, H., 1980. The geochemistry of n-alkanes with an even-odd
1038   predominance in the Tertiary Shahejie Formation of northern China. Physics and Chemistry
1039   of the Earth, Proceedings of the Ninth International Meeting on Organic Geochemistry 12,
1040   115–121. https://doi.org/10.1016/0079-1946(79)90093-4

1041 Simoneit, B.R.T., 1977. Diterpenoid compounds and other lipids in deep-sea sediments and their
1042   geochemical significance. Geochimica et Cosmochimica Acta 41, 463–476.
1043   https://doi.org/10.1016/0016-7037(77)90285-X

1044 Sinninghe Damsté, J.S., Kenig, F., Koopmans, M.P., Köster, J., Schouten, S., Hayes, J.M., de Leeuw,
1045   J.W., 1995. Evidence for gammacerane as an indicator of water column stratification.
1046   Geochimica et Cosmochimica Acta 59, 1895–1900. https://doi.org/10.1016/0016-
1047   7037(95)00073-9

1048 Sinninghe Damsté, J.S., Schouten, S., van Duin, A.C.T., 2001. Isorenieratene derivatives in sediments:
1049   possible controls on their distribution. Geochimica et Cosmochimica Acta 65, 1557–1571.
1050   https://doi.org/10.1016/S0016-7037(01)00549-X

1051 Sinninghe Damsté, J.S., Wakeham, S.G., Kohnen, M.E.L., Hayes, J.M., de Leeuw, J.W., 1993. A 6,000–
1052   year sedimentary molecular record of chemocline excursions in the Black Sea. Nature 362,
1053   827–829. https://doi.org/10.1038/362827a0

1054 Słama, S., 2019. Chemical characteristics and origin of crude oil from the Boulby Mine (NE England)
1055   based on analysis of the saturated hydrocarbon fraction. BSc thesis, University of Warsaw,
1056   42p.

1057 Słowakiewicz, M., 2016. Characteristic biomarkers in organic matter from three Zechstein (Late
1058   Permian) carbonate units. Zeitschrift der Deutschen Gesellschaft für Geowissenschaften 167,
1059   269–279. https://doi.org/10.1127/zdgg/2016/0061

1060 Słowakiewicz, M., Blumenberg, M., Więcław, D., Röhling, H.-G., Scheeder, G., Hindenberg, K., Leśniak,
1061   A., Idiz, E.F., Tucker, M.E., Pancost, R.D., Kotarba, M.J., Gerling, J.P., 2018. Zechstein Main
1062   Dolomite oil characteristics in the Southern Permian Basin: I. Polish and German sectors.
1063   Marine and Petroleum Geology 93, 356–375.
1064   https://doi.org/10.1016/j.marpetgeo.2018.03.023

1065 Słowakiewicz, M., Gąsiewicz, A., 2013. Palaeoclimatic imprint, distribution and genesis of Zechstein
1066   Main Dolomite (Upper Permian) petroleum source rocks in Poland: Sedimentological and

1067   geochemical rationales. Geological Society, London, Special Publications 376, 523–538.
1068   https://doi.org/10.1144/SP376.21

1069 Słowakiewicz, M., Tucker, M.E., Hindenberg, K., Mawson, M., Idiz, E.F., Pancost, R.D., 2016.
1070   Nearshore euxinia in the photic zone of an ancient sea: Part II – The bigger picture and
1071   implications for understanding ocean anoxia. Palaeogeography, Palaeoclimatology,
1072   Palaeoecology 461, 432–448. https://doi.org/10.1016/j.palaeo.2016.09.003

1073 Słowakiewicz, M., Tucker, M.E., Vane, C.H., Harding, R., Collins, A., Pancost, R.D., 2015. Shale-gas
1074   potential of the mid-Carboniferous Bowland-Hodder unit in the Cleveland Basin (Yorkshire)
1075   Central Britain. Journal of Petroleum Geology 38, 59–75. https://doi.org/10.1111/jpg.12598

1076 Smith, D.B., 1989. The late Permian palaeogeography of north-east England. Proceedings of the
1077   Yorkshire Geological and Polytechnic Society 47, 285–312.
1078   https://doi.org/10.1144/pygs.47.4.285

1079 Smith, D.B., Francis, E.A., 1967. Permian and Trias, in: Smith, D.B., Francis, E.A., Calver, M.A., Gaunt,
1080   G.D., Pattison, J., Edwards, A.H., Harrison, R.K. (Eds.), Geology of the Country between
1081   Durham and West Hartlepool, Memoirs of the Geological Survey of Great Britain, England
1082   and Wales. pp. 90–186.

1083 Smith, D.B., Harwood, G.M., Pattison, J., Pettigrew, T.H., 1986. A revised nomenclature for Upper
1084   Permian strata in eastern England. Geological Society, London, Special Publications 22, 9–17.
1085   https://doi.org/10.1144/GSL.SP.1986.022.01.02

1086 Smith, K., Smith, N.J.P., Holliday, D.W., 1985. The deep structure of Derbyshire. Geological Journal 20,
1087   215–225. https://doi.org/10.1002/gj.3350200303

1088 Sofer, Z., 1984. Stable carbon isotope compositions of crude oils; application to source depositional
1089   environments and petroleum alteration. AAPG Bulletin 68, 31–49.

1090 Song, J., 2015. Shale oil potential and depositional environment of the Lower Toarcian Posidonia
1091   Shale in NW Europe. Publikationsserver der RWTH Aachen University.

1092 Song, J., Littke, R., Weniger, P., Ostertag-Henning, C., Nelskamp, S., 2015. Shale oil potential and
1093   thermal maturity of the Lower Toarcian Posidonia Shale in NW Europe. International Journal
1094   of Coal Geology 150–151, 127–153. https://doi.org/10.1016/j.coal.2015.08.011

1095 Steele, R.P., 1983. Longitudinal draa in the Permian Yellow Sands of North-East England, in:
1096   Brookfield, M.E., Ahlbrandt, T.S. (Eds.), Developments in Sedimentology. Elsevier, pp. 543–
1097   550. https://doi.org/10.1016/S0070-4571(08)70812-4

1098 Summons, R.E., Powell, T.G., 1986. Chlorobiaceae in Palaeozoic seas revealed by biological markers,
1099   isotopes and geology. Nature 319, 763–765. https://doi.org/10.1038/319763a0

1100 Sun, Y., Sheng, G., Peng, P., Fu, J., 2000. Compound-specific stable carbon isotope analysis as a tool
1101   for correlating coal-sourced oils and interbedded shale-sourced oils in coal measures: an
1102   example from Turpan basin, north-western China. Organic Geochemistry 31, 1349–1362.
1103   https://doi.org/10.1016/S0146-6380(00)00069-3

1104 Taylor, J.C.M., 1998. Upper Permian - Zechstein, in: Glennie, K.W. (Ed.), Petroleum Geology of the
1105   North Sea. Blackwell Science Ltd, pp. 174–211.

1106 Ten Haven, H.L., De Leeuw, J.W., Schenck, P.A., 1985. Organic geochemical studies of a Messinian
1107   evaporitic basin, northern Apennines (Italy) I: Hydrocarbon biological markers for a
1108   hypersaline environment. Geochimica et Cosmochimica Acta 49, 2181–2191.
1109   https://doi.org/10.1016/0016-7037(85)90075-4

1110 Thompson, K.F.M., 1987. Fractionated aromatic petroleums and the generation of gas-condensates.
1111   Organic Geochemistry 11, 573–590. https://doi.org/10.1016/0146-6380(87)90011-8

1112 Thompson, K.F.M., 1983. Classification and thermal history of petroleum based on light
1113   hydrocarbons. Geochimica et Cosmochimica Acta 47, 303–316.
1114   https://doi.org/10.1016/0016-7037(83)90143-6

1115 Underhill, J.R., 2003. The tectonic and stratigraphic framework of the United Kingdom's oil and gas
1116   fields. Geological Society, London, Memoirs 20, 17–59.
1117   https://doi.org/10.1144/GSL.MEM.2003.020.01.04

1118 Underhill, J.R., Monaghan, A.A., Browne, M.A.E., 2008. Controls on structural styles, basin
1119   development and petroleum prospectivity in the Midland Valley of Scotland. Marine and
1120   Petroleum Geology 25, 1000–1022. https://doi.org/10.1016/j.marpetgeo.2007.12.002
1121 van Buchem, F.S.P., Knox, R.W.OB., 1998. Lower and Middle Liassic Depositional Sequences of
1122   Yorkshire (U.K.), in: Graciansky, P.-C. de, Hardenbol, J., Jacquin, T., Vail, P.R. (Eds.), Mesozoic
1123   and Cenozoic Sequence Stratigraphy of European Basins. SEPM Special Publication, pp. 545–
1124   559. https://doi.org/10.2110/pec.98.02.0545
1125 van Kaam-Peters, H.M.E., Schouten, S., de Leeuw, J.W., Sinninghe Damsté, J.S., 1997. A molecular
1126   and carbon isotope biogeochemical study of biomarkers and kerogen pyrolysates of the
1127   Kimmeridge Clay Facies: palaeoenvironmental implications. Organic Geochemistry 27, 399–
1128   422. https://doi.org/10.1016/S0146-6380(97)00084-3
1129 Walters, C.C., Lillis, P.G., Peters, K.E., 2012. Molecular indicators of geothermal history, in: Harris,
1130   N.B., Peters, Kenneth E. (Eds.), Analyzing the Thermal History of Sedimentary Basins:
1131   Methods and Case Studies, SEPM Special Publication. Tulsa, pp. 17–28.
1132   https://doi.org/10.2110/sepmsp.103
1133 Waples, D.W., Machihara, R., 1991. Biomarkers for geologists: a practical guide to the application of
1134   steranes and triterpanes in petroleum geology, AAPG Methods in Exploration Series 9, 91p.
1135 Wenger, L.M., Davis, C.L., Isaksen, G.H., 2002. Multiple controls on petroleum biodegradation and
1136   impact on oil quality. SPE Reservoir Evaluation & Engineering 5, 375–383.
1137   https://doi.org/10.2118/80168-PA
1138 Woods, P.J.E., 1979. The geology of Boulby Mine. Economic Geology 74, 409–418.
1139   https://doi.org/10.2113/gsecongeo.74.2.409
1140 Woods, P.J.E., 1973. Potash exploration in Yorkshire: Boulby Mine pilot borehole. Transactions of the
1141   Institute of Minerals and Metallurgical Transactions 82B, 99–106.

1142

1143

1144

1145

1146

1147

1148

1149

1150

1151

1152

1153

1154

Sample no	C_{27} Ts/Tm	M/H	C_{29} 20S	C_{29} ββ	TA(I)/ TA(I+II)	MPI 1	Rc	MDR	Rm
1	0.41	0.12	0.52	0.56	0.07	0.65	0.79	4.88	0.87
2	nd	nd	nd	nd	nd	1.39	1.23	nd	nd
3	nd	nd	nd	nd	nd	1.3	1.18	nd	nd
4	nd	nd	nd	nd	nd	1.33	1.2	nd	nd
Malton 4	0.52-0.71 (0.6)	0.03-0.13 (0.07)	0.46-0.57 (0.51)	0.45-0.58 (0.51)	0.25-0.33 (0.29)	0.7-0.81 (0.75)	0.7-0.81 (0.75)	1.78-2.02 (1.9)	0.64-0.66 (0.65)

1155

1156 Table 1. Biomarker and non-biomarker maturity parameters for Boulby oil (samples 1-4) and Malton

1157 4 KAF samples. nd – not determined. Numerator gives range of values and denominator gives average

1158 values.

1159 C_{27} Ts/Tm – C_{27} 18α-trisnorneohopane/17α-trisnorhopane

1160 M/H – moretane/hopane

1161 C_{29} 20S – 20S/(20S + 20R) epimers of 5α(H),14α(H),17α(H)-ethylsterane

1162 C_{29} ββ – 5α(H),14β(H),17β(H)/[5α(H),14β(H),17β(H) + 5α(H),14α(H),17α(H) 20R ethylsteranes]

1163 TA(I)/TA(I + II) – TA(I) = C_{20} + C_{21}, TA(II)=ΣC_{26}-C_{28} (20S + 20R) triaromatic steroids

1164 MPI 1 – methylphenanthrene index = $1.5 \times (2\text{-MP} + 3\text{-MP})/P + 1\text{-MP} + 9\text{-MP}$

1165 Rc – calculated vitrinite reflectance = $0.40 + 0.60 \times$ MPI 1

1166 MDR – methyldibenzothiophene ratio = 4-MDBT/1-MDBT

1167 R_m – calculated vitrinite reflectance = $0.073 \times$ MDR + 0.51

1168

Sample	density [g/cm^3]	$\delta^{13}C_{SAT}$	$\delta^{13}C_{ARO}$	CV
1	0.84617	-25.2	-24.4	-2.06
2	0.80984	-24.25	-22.61	-0.49
3	0.84487	-24.04	-22.58	-0.96
4	0.81543	-23.92	-23.37	-3.01

1169

1170 Table 2. Density and stable carbon isotopic composition of the saturated ($\delta^{13}C_{SAT}$, ‰) and aromatic

1171 ($\delta^{13}C_{ARO}$, ‰) fractions of Boulby oil (samples 1-4). CV – canonical variable (CV = $-2.53\delta^{13}C_{SAT}$ +

1172 $2.22\delta^{13}C_{ARO}$ – 11.65; after Sofer, 1984).

1173

Sample no	Pr/Ph	Pr/n-C_{17}	Ph/n-C_{18}	C_{19}/C_{23}	C_{24Tet}/C_{23}	C_{29}/H	C_{30dia}/H	C_{31}R/H
1	0.71	0.54	0.78	0.07	0.07	0.27	0.09	0.39
2	0.71	0.27	0.53	nd	nd	nd	nd	nd

3	0.72	0.28	0.54	nd	nd	nd	nd	nd
4	0.71	0.28	0.54	nd	nd	nd	nd	nd
Malton 4	$\dfrac{0.3-0.46}{(0.38)}$	$\dfrac{0.17-0.58}{(0.42)}$	$\dfrac{0.21-0.58}{(0.51)}$	$\dfrac{0.03-0.24}{(0.08)}$	$\dfrac{0.14-0.58}{(0.31)}$	$\dfrac{0.49-1.17}{(0.74)}$	nd	$\dfrac{0.31-0.52}{(0.4)}$

1174

1175   Table 3a. Source-related geochemical characteristics of Boulby oil (samples 1-4) and Malton 4

1176   dolomite samples. nd – not determined. Numerator gives range of values and denominator gives

1177   average values.

1178

HHI	$C_{32(S+R)}/C_{31(S+R)}$	$C_{34(S+R)}/C_{33(S+R)}$	$C_{35}S/C_{34}S$	$C_{27}dia$	$C_{29}dia$	$\%C_{27}$	$\%C_{28}$
0.14	1.3	1.35	0.8	0.33	0.69	39	25
nd	nd	nd	nd	0.49	nd	13	nd
nd	nd	nd	nd	0.72	nd	12	nd
nd	nd	nd	nd	0.94	nd	9	nd
$\dfrac{0.09-0.3}{(0.21)}$	$\dfrac{0.82-1.43}{(1.02)}$	$\dfrac{0.63-1.88}{(0.98)}$	$\dfrac{0.45-1.79}{(1.23)}$	$\dfrac{0.75-4.33}{(1.7)}$	$\dfrac{0.28-2.48}{(0.77)}$	$\dfrac{31-44}{(38)}$	$\dfrac{24-27}{(26)}$

1179

1180   Table 3b. Continued.

1181

$\%C_{29}$	C_{27}/C_{29}	C_{28}/C_{29}	tricyclics/17α-hopanes	steranes/17α-hopanes	DBT/P	CPI
36	1.09	0.871	0.03	0.25	0.49	0.98
87	nd	nd	nd	nd	0.36	0.99
88	nd	nd	nd	nd	0.42	1.02
91	nd	nd	nd	nd	0.26	0.99
$\dfrac{29-42}{(36)}$	$\dfrac{0.75-1.53}{(1.08)}$	$\dfrac{0.6-0.91}{(0.72)}$	$\dfrac{0.14-1.19}{(0.67)}$	$\dfrac{0.12-0.37}{(0.23)}$	$\dfrac{0.86-1.34}{(1.16)}$	$\dfrac{0.83-1.01}{(0.95)}$

1182

1183   Table 3c. Continued.

1184

1185   Pr/Ph – pristane/phytane.

1186   Pr/n-C_{17} – pristane/n-heptadecane.

1187   Ph/n-C_{18} – phytane/n-octadecane.

1188 C_{19}/C_{23} – C_{19}/C_{23} tricyclic terpanes.

1189 C_{22}/C_{21} – C_{22}/C_{21} tricyclic terpanes.

1190 C_{24Tet}/C_{23} – C_{24} tetracyclic/C_{23} tricyclic terpanes.

1191 C_{29}/H – C_{29} norhopane/C_{30} 17α-hopane.

1192 C_{30} dia/H – C_{30} diahopane/C_{30} 17α-hopane.

1193 C_{31} R/H – C_{31} homohopane 22R/C_{30} 17α-hopane.

1194   HHI – homohopane index: C_{35}αβ(S + R)/(ΣC_{31}-C_{35}αβ S + R).

1195 C_{32}/C_{31} (S + R) – C_{32} (S + R) 17α-hopane/C_{31} (S + R) 17α-hopane.

1196 C_{34}/C_{33} (S + R) – C_{34} (S + R) 17α-hopane/C_{33} (S + R) 17α-hopane.

1197 $C_{35}S/C_{34}S$ - $C_{35}S/C_{34}S$ homohopanes.

1198 C_{27} dia – diasterane/sterane ratio – C_{27} 13β,17α(H) (20S + 20R)/(C_{27} 5α,14α,17α(H) 20S + 20R +

1199   5α,14β,17β(H) 20S + 20R).

1200 C_{29} dia – diasterane/sterane ratio – C_{29} 13β,17α(H) (20S + 20R)/(C_{29} 5α,14α,17α(H) 20S + 20R +

1201   5α,14β,17β(H) 20S + 20R).

1202   %C_{27} (m/z 217) – $100 \times C_{27}S/(C_{27}S + C_{28}S + C_{29}S)$.

1203   %C_{28} (m/z 217) – $100 \times C_{28}S/(C_{27}S + C_{28}S + C_{29}S)$.

1204   %C_{29} (m/z 217) – $100 \times C_{29}S/(C_{27}S + C_{28}S + C_{29}S)$.

1205 C_{27}/C_{29} – C_{27}/C_{29} sterane ratio.

1206 C_{28}/C_{29} – C_{28}/C_{29} sterane ratio.

1207   Tricyclics/17α-hopanes – ΣC_{19-26} tricyclic terpanes/(ΣC_{19-26} tricylic terpanes + ΣC_{29-35} 17α-hopanes).

1208   Steranes/17α-hopanes – ΣC_{27-29} regular steranes/ΣC_{29-35} 17α-hopanes.

1209   DBT/P – dibenzothiophene/phenanthrene.

1210   CPI – carbon preference index based on n-alkanes [$\Sigma(C_{25}$-$C_{33})$odd/$\Sigma(C_{24}$-$C_{32})$even + $\Sigma(C_{25}$-

1211 $C_{33})$odd/$\Sigma(C_{26}$-$C_{34})$even]/2.

1212

Highlights

- A new and working petroleum source rock on the UK Continental Shelf

- Boulby oil seeping from rock-salt fractures derives from sapropelic dolomite

- A carbonate-evaporite depositional setting is confirmed

Declaration of interests

☒ The authors declare that they have no known competing financial interests or personal relationships that could have appeared to influence the work reported in this paper.

☐The authors declare the following financial interests/personal relationships which may be considered as potential competing interests: